FELIPE TIAGO E SILVA MENEZES

REMOTE SENSING TECHNIQUES IN THE ANALYSIS OF CHANGE DETECTION IN THE ALGARVE COAST, PORTUGAL

UAlg
UNIVERSIDADE DO ALGARVE

FACULDADE DE CIÊNCIAS E TECNOLOGIA

2022

FELIPE TIAGO E SILVA MENEZES

REMOTE SENSING TECHNIQUES IN THE ANALYSIS OF CHANGE DETECTION IN THE ALGARVE COAST, PORTUGAL

Master in Marine and Coastal Systems

Work performed under the supervision of:

Prof. Doutor Fernando Miguel Granja Martins (UALG)

Prof. Doutora Helena Maria Neto Paixão Vazquez Fernandez (UALG)

UAlg

UNIVERSIDADE DO ALGARVE

FACULDADE DE CIÊNCIAS E TECNOLOGIA

2022

Declaração de autoria de trabalho / Declaration of Authorship of work

Application of remote sensing techniques in monitoring vegetation and land use in the Littoral do Algarve

Declaro ser o(a) autor(a) deste trabalho, que é original e inédito. Autores e trabalhos consultados estão devidamente citados no texto e constam da listagem de referências incluída.

I declare to be the author of this work, which is original and unpublished. Authors and works consulted are duly cited in the text and are included in the list of references.

X_____

FELIPE TIAGO E SILVA MENEZES

FARO, 31 / 03 / 2022

COPYRIGHT

Acknowledgements:

First, I thank God for giving me the strength to face this challenge.

The journey was not easy. Several falls and stumbles along the way, but giving up was never an option, even with the world falling apart in this dark pandemic and wars period that the world faces today.

I want to thank my family, My Wife Cindel Borba, My little daughter Olivia, who was still in the womb as I wrote this, but for whom all the attention, love and affection, effort, and sacrifice are worth it. To my Parents, Mr. Oscar Menezes, and Mrs. Yanara Menezes, for all their support and advice during all these years.

To my dear professors Fernando Martins and Helena Martins, I owe everything I know about Remote Sensing and Geographic Information Systems: thank you very much for always being available to help me with this.

My wish is that faith hope will be renewed.

“Et cognoscetis veritatem, et veritas liberabit vos”

Abstract

The process of occupation in the Algarve area is millenary. The last decades have shown that economic activities in the region have caused significant changes in the use and occupation of the land. The main objective of this study was to correlate carbon sequestration and the evolution of land use and occupation, in the coastal zone of Algarve, Portugal, through the application of vegetation indices such as NDVI, PRI, CO_{2f}lux, compared with MODIS GPP and COPERNICUS Corine Land Cover, between the years 1990 and 2020. The results were expressed through digital cartography for better data visualization. The NDVI results demonstrate that the vigor and biomass produced by the coastal vegetation tended to increase. There was a decrease in areas without vegetation and areas with sparse vegetation, which were replaced mainly by the vegetation of moderate density and, secondly, by the vegetation of high density. The joint analysis of the indexes corroborates such results, PRI and CO2flux, which, related in a linear regression with the MODIS GPP, indicated that the study region has a great capacity to store carbon, mainly on the West Coast, where the highest density was observed of biomass and a consequent higher level of GPP. The results also indicated an abandonment of rural areas, which were taken over by vegetation and urban sprawl, as well as a growth of around 69% in areas destined for leisure areas, such as golf courses. The results also showed that the environmental preservation areas in the region, the RAMSAR and REDE NATURA 2000 Sites, did not suffer from changes in the use and occupation of their areas.

Keywords: Remote Sensing, GIS, geospatial analysis, Corine Land Cover, Vegetation indices, Algarve.

Resumo

É milenar o processo de ocupação na zona do Algarve. As últimas décadas mostraram que as atividades económicas da região têm provocado significativas alterações no uso e ocupação do Solo. O principal objetivo deste estudo foi correlacionar o sequestro de carbono e a evolução do uso e ocupação do solo, na zona costeira do Algarve, Portugal, através da aplicação de índices de vegetação como NDVI, PRI, CO_2flux, comparados com os produtos MODIS GPP e COPERNICUS Corine Land Cover, entre os anos de 1990 e 2020. Os resultados foram expressos através cartografia digital para melhor visualização dos dados. Os resultados do NDVI demonstram que o vigor e biomassa produzidos pela vegetação litorânea tendeu a crescer. Houve uma diminuição das áreas sem vegetação e das áreas de vegetação esparsa, que foram substituídas, principalmente, por uma vegetação de densidade moderada e, em segundo lugar, por uma vegetação de alta densidade. Tais resultados são corroborados pela análise conjunta dos índices , PRI e CO2flux, que, relacionado numa regressão linear com os MODIS GPP, indicou que região de estudo tem uma grande capacidade de estocar de carbono, principalmente na Costa Oeste, onde foi observado a maior densidade de biomassa e consequente maior nível de GPP. Os resultados também indicaram que houve um abandono das áreas rurais, que foram tomadas pela vegetação e pela expansão urbana. Assim como um crescimento de cerca de 69% das áreas destinadas às zonas de lazer, como os campos de Golfe. Os resultados ainda mostraram que as áreas de preservação ambiental da região, os Sítios RAMSAR E REDE NATURA 2000, não sofreram com as alterações do uso e ocupação de suas áreas.

Palavras Chaves: Deteção Remota, SIG, análise geoespacial, Corine Land Cover, índices de Vegetação, Algarve.

Resumo Expandido

Registos arqueológicos comprovam que a ocupação da região algarvia remonta um período de mais de 3 mil anos. Civilizações como a dos fenícios, Romanos e, posteriormente, a de Cristãos e Muçulmanos, alternaram-se no controlo da região. Isto indica que as condições pristinas ambientais foram bastante comprometidas ao longo dos séculos. Nas últimas décadas, o turismo, caracterizado como uma das principais atividades económicas da região, tem experimentado uma grande expansão. Tal expansão, tem refletido diretamente no uso e ocupação do solo, sendo a região litorânea o grande foco dos maiores investimentos, Nessa perspetiva, uma das áreas das ciências ambientais que tem se destacado é a Deteção Remota. O advento de novas gerações de satélites, equipados com sensores de alta resolução, possibilitou novas missões voltadas ao monitoramento de sistemas marinhos e costeiros, em escala local, regional e global. As abordagens dessas técnicas podem ser realizadas qualitativa ou quantitativamente, para obter informações sobre os processos que envolvem o ambiente abiótico e biótico, como índices de clorofila, sólidos suspensos, ciclo do carbono, temperatura da superfície do mar, topografia e fenologia. A capacidade de prever respostas ecológicas tornou-se cada vez mais importante. Portanto, as técnicas de "Change Detection" visam monitorar, identificar e analisar problemas ambientais por meio de imagens obtidas de satélites no mesmo local, em um determinado período. Essas técnicas, associada ao monitoramento da sazonalidade do ciclo do carbono, facilita o entendimento dos efeitos das mudanças climáticas futuras, que podem afetar a homeostase ecológica. Neste trabalho foram aplicados Índices de Vegetação, uma das ferramentas mais utilizadas, capazes de analisar diretamente as mudanças dos padrões do uso e ocupação do solo. O índice da Diferença Normalizada (NDVI). é um indicador importante a ser utilizado na deteção de mudanças na cobertura vegetal para diferentes períodos em uma mesma área, por meio da determinação da densidade da fitomassa foliar por unidade de área Este índice, combinado com o Índice de Refletância Fotoquímica (PRI), que é um método utilizado em estudos de estresse e produtividade da vegetação, por meio da eficiência fotossintética da vegetação. Também é utilizado o índice de fluxo de CO_2, que correlaciona os índices de vegetação mencionados acima, para entender a relação entre o estoque e o sequestro de carbono (Baptista, 2003). Outro parâmetro é a produção primária bruta (GPP), usada para quantificar o valor de biomassa de um ecossistema ao longo do tempo, e é a soma da fixação de C bruto por organismos autotróficos por unidade, que em outras palavras, representa a taxa de carbono total fotossintetizada pelas plantas. Este trabalho também utilizou dados do Corine Land Cover, projeto desenvolvido pela União Europeia, afim e coletar de dados de cobertura do solo baseado em inventários cartográficos. De acordo com o que foi exposto até agora, o objetivo deste estudo foi descrever a evolução da biomassa da

vegetação costeira no Algarve, bem como a evolução do uso e ocupação do solo, correlacionada com a produção primária bruta de CO_2, expressa em cartografia digital. A evolução de tais fatores foi baseada em técnicas de Deteção de Mudanças na Cobertura do Solo por Sensoriamento Remoto suportadas por técnicas de SIG. Para atingir o objetivo maior, os seguintes objetivos secundários são abordados: aplicação de Índices de Vegetação como NDVI, PRI, *sPRI* e CO2flux por meio de uma série temporal de imagens LANDSAT de 1990 a 2020 e MODIS GPP de 2002 até 2020, além de cálculo de Change Detection de Cobertura do solo por meio do programa Copernicus Corine Land Cover em uma série temporal de 1990 a 2018 para fins de comparação e validação de dados; elaboração de Mapas Digitais através da aplicação de técnicas GIS. Os resultados deste trabalho revelaram que na zona de estudo, ocorreu a diminuição de áreas sem vegetação e vegetação esparsa, compensada, por outro lado, pelo aumento de áreas com vegetação moderada e densa, indicam um ganho notável de biomassa e vigor vegetativo para a região de estudo, ambos no contexto geral e para a Ria Formosa, visto que o parque também segue o mesmo padrão de percentagens de classes de vegetação. Consequentemente, pode-se dizer que a vegetação não se encontra atualmente em um estágio de estresse hídrico extremo. A corroborar com os dados obtidos com NDVI, as análises de PRI, Co_2Flux e MODIS GPP apontam também para uma variação cíclica na produção de Biomassa e vigor da vegetação ao longo do Litoral do Algarve. E ao analisar os gráficos e respetivos mapas, foi possível observar que a região é um grande reservatório de carbono. Observou-se também que houve diminuição da eficiência do processo de sequestro de carbono, em áreas urbanas, onde a concentração de vegetação é menor. Tais resultados validam e corroboram com os níveis de NDVI distribuídos pela zona de estudo, que se mostram menores nas áreas urbanas. Tanto para o GPP quanto para o Co_2Flux, os valores se aproximaram dos níveis de concentração elevados, principalmente da região da costa oeste, no sítio homólogo NATURA 2000, o que pode indicar que a localização é homeostase ecológica e que as políticas de preservação pública, que foram aqui discutidas anteriormente, são sendo seguido. Ao observar os mapas de distribuição dos valores de Co_2flux para 1990 e 2020, notamos que eles permaneceram em níveis intermediário e baixo, em áreas suscetíveis a inundações e, portanto, pode-se inferir que isso se deve justamente ao movimento da maré no momento em que os dados foram coletados pelos satélites. Vale ressaltar que na análise dos índices de vegetação em zonas úmidas costeiras, ainda é difícil ter precisão exata de medição devido à variação da maré. O aumento dos níveis de produção de biomassa na área de estudo ao longo do período medido pode estar diretamente relacionado à mudança nos níveis de precipitação, contribuindo assim positivamente para a entrada de nutrientes essenciais como N e P através de ciclos biogeoquímicos, favorecendo o crescimento da vegetação, e, consequente maior eficiência fotossintética. A análise do CORINE LAND COVER revelou que as áreas ocupadas por vegetação cresceram aproximadamente 4% em três décadas; as áreas destinadas à agricultura diminuíram cerca de 13.5%; e as áreas urbanas cresceram cerca de 6,5%. Ao analisar esses resultados, é possível deduzir que

as áreas antes destinadas à agricultura, deram lugar a áreas urbanizadas, ou que foram abandonadas, o que deu lugar ao processo de sucessão ecológica, que gradativamente fez com que a vegetação natural ocupasse o espaço das áreas anteriormente utilizadas para agricultura. Ao analisar os dados referentes ao uso de ocupação do solo nas áreas destinadas à proteção ambiental, os Sítios RAMSAR e NATURA 2000, presentes no Litoral Algarvio, como Sapais de Castro Marim, Ria Formosa, Ria de Alvor e Sítio Natura 2000 na Costa Oeste, nota-se que não houve alteração significativa em termos de diminuição de hectares, até 2018, ano passado com dados oficiais publicados e disponíveis para o projeto CORINE LAND COVER. Infere-se, então, que os programas coordenados pela União Europeia estão a ser respeitados, evitando-se assim a exploração do solo para fins agrícolas, de infraestruturas de lazer ou em detrimento de zonas urbanas. Neste trabalho, foi utilizada uma abordagem multidisciplinar, que envolveu técnicas de Sensoriamento Remoto, Técnicas de Sistemas de Informação Geográfica, Análise Geoespacial, Princípios de Biologia e Ecologia para toda a zona Litoral do Algarve. Até onde se sabe, esta combinação analítica não havia sido realizada até o momento para a área de estudo. Nas zonas Litorâneas e costeiras, a deteçao Remota e os Sistemas de informação geográfica são cada vez mais utilizados como ferramenta de apoio que permite homogeneizar e integrar toda a informação disponível numa geodatabase, aceder a dados, gerar cartografia temática e efetuar análises espaciais e geoestatísticas. Essas ferramentas permitem análises geoestatísticas, edição e automação de dados, visualização, mapeamento e tarefas baseadas em mapas, consulta espacial, análise espacial, etc. Neste sentido, os resultados aqui apresentados, são de grande importância para que decisores e políticos se possam basear no planeamento de ações mitigadoras em prol do meio ambiente, de forma que a região costeira algarvia seja preservada para as gerações futuras.

Palavras Chaves: Deteção Remota, SIG, Change Detection, Análise geoespacial, Corine Land Cover, Índices de Vegetação, Algarve.

Table of Contents

LIST OF ABBREVIATIONS

μm - Micrometer

$\rho BLUE$ - Reflectance for the blue band

$\rho GREEN$- Reflectance for the green band

ρk - Spectral reflectance

ρMIR - Mid-infrared band reflectance

ρNIR - Near infrared band reflectance

ρRED - Red band reflectance

θ - Sun's zenith angle

C - Carbon

CLC - Corine Land Cover

CO^2 - Carbon Dioxide

CO2flux - Carbon Flux

d^2- Earth-Sun Distance in Astronomical Units

DN - Digital Level

EMR- Electromagnetic Radiation

EOS - Earth Observation System

ERTS - Earth Resources Technology Satellite

ESA - European Space Agency

ETM - Enhanced Thematic Mapper

ETM+ - Enhanced Thematic Mapper Plus

FPAR - Fraction of Photosynthetically Active Radiation

gC/m^2 – grams of carbon per square meter

GPP - Gross Primary Production

ha – Hectares

HDF - Hierarchical Data Format

ICNF - Institute for Nature and Forest Conservation

ICZM -Integrated Coastal Zone Management

IPAR – Intercepted photosynthetically active radiation

k - Exoatmospheric solar radiance

KgC/m^2 - Kilogram of carbon per square meter

GIS - Geographic Information Systems

Landsat - Land Remote Sensing Satellite

LC – Land cover

LU- Land use

Lλ - Spectral Radiance

Lmax - Maximum spectral radiance calibration coefficient

Lmin - Minimum spectral radiance calibration coefficient

m^2 – square meter

MJ/m^2 - Megajoule per square meter

MODIS - Moderate Resolution Imaging Spectroradiometer

MOD17 - MODIS Primary Productivity Products

MSS - Multispectral Scanner

MYD17A2H – Modis/Aqua Gross Primary Production 8-Day L4

NASA - National Aeronautics and Space Administration

NDVI – Normalized Difference Vegetation Index

OLI - Operational Land Imager

PRI - Photochemical Reflectance Index

shp – shapefile format

RBV- Return Beam Vidicon

RS- Remote Sensing

Tiff. – Tagged Image File Format

TIRS - Thermal Infrared Sensor

TIRS-2 -Thermal Infrared Sensor-2

TM - Thematic Mapper

USGS - United States Geological Survey

UTM - Universal Transverse Mercator

WGS - World Geodetic System

Wm^{-2} μm^{-1} - Watt per square meter per micrometer

List of Figures

List of Tables

1 INTRODUCTION

The Algarve region, situated in the south of Portugal, has archaeological records that indicate the occupation of its lands by civilizations from the pre-Roman eras, dating back to the 4th century BC. Its geopolitical importance in the Roman Empire, integrated into the Atlantic Route, responsible for a continuous flow of people and goods, established the region as an important commercial centre. The later Muslim occupation of the Iberian Peninsula from century VIII was crucial for a break with the rest of Western Europe in all aspects of the sphere of society, reflected in the economics, politics, culture, and religion, which are perceptible until today (Bernardes, 2011; Viegas, 2011; Ignacio de la Torre, 2020).

From this premise, it is possible to affirm that the human presence in the region has been changing land use for millennia. Martins (2016), quoting Zachar (1982), affirms that: "The Mediterranean region is characterized by having seasonal climate and specific ecological and edaphic conditions that make it one of the most vulnerable ecosystems in Europe, this is, namely, due to the fragility of the ecosystems and the low rates of biomass production during dry periods." Currently, the facts about the conjunction of ecosystems inserted in the Algarve biomes are well known. Consequently, environmental management has been the focus of many public policies, debates, and research groups, committed to understanding and describing all the processes and factors involved in the evolution of regional ecological systems, as well as developing mitigating and preventive measures concerning soil conservation and deceleration of the desertification process that can become irreversible, as already reported in other areas of the Mediterranean region (Martins, 2016).

From this perspective, one of the areas of environmental sciences that have reached a prominent relevance is Remote Sensing. The advent of new generations of satellites equipped with high-resolution sensors enabled new missions to monitor marine and coastal systems on a local, regional, and global scale. The approaches of these techniques can be carried out qualitatively or quantitatively to obtain information on the processes that involve the abiotic and

biotic environment, such as chlorophyll indices, suspended solids, carbon cycle, sea surface temperature, topography, and phenology (Pettorelli *et al.,* 2005; Tuia *et al.,* 2016; INPE, 2019).

The ability to predict ecological responses has become increasingly important. Therefore, Change Detection techniques aim to monitor, identify, and analyze environmental problems through images obtained from satellites in the exact location over a specific period. This technique, associated with monitoring the seasonality of the carbon cycle, facilitates the understanding of the effects of future climate changes, which can affect ecological homeostasis (Asokan & Anitha, 2019).

One of the most used tools to analyze these factors is the direct application of vegetation indexes difference within the Change Detection techniques. These data are obtained from the calculation of indices such as the Normalized Difference Vegetation Index (NDVI), which is an important indicator to be used in the detection of changes in vegetation cover for different periods in the same area by determining the density of leaf phytomass per unit area (Melo *et al.*, 2011). This index is combined with the Photochemical Reflectance Index (PRI), a method used in studies of vegetation stress and productivity, through the photosynthetic efficiency of vegetation (da Rocha Almeida & da Silva Rocha, 2018). In addition, the CO_2flux index is also used, which correlates with the vegetation indices mentioned above, to understand the relationship between the stock and carbon sequestration (Baptista, 2003). Another parameter is the Gross primary production (GPP), used to quantify the biomass value of an ecosystem over time, and it is the sum of gross C fixation by autotrophic organisms per unit, which in other words, represents the total carbon rate photosynthesized by plants (Myneni *et al.*, 1995).

The literature focused on implementing the Change Detection techniques is vast and covers topics from climate footprint to issues that concern the socio-economic sphere. Below are some works carried out in recent years for their most everyday purposes.

Recent studies in the Iberian Peninsula used the resources of the NDVI index to investigate issues related to droughts at regional and global scales. For example, Vicente-Serrano *et al.* (2013) evaluated the responses of terrestrial biomes by correlating the drought rate and the indicators of activity and growth of vegetation (Gouveia *et al.,* 2009; Bastos *et al.,* 2016) analyzed the impacts of drought on vegetation in the Mediterranean Base. The correlation of drought regimes and fires in Portugal was also studied considering different satellite data sets (Parente *et al.,* 2019; Teodoro & Amaral, 2019). Also linked to this theme, MODIS indicators were applied to improve the detection of forest fires in Portugal (Marcos *et al.,* 2019).

Studies focusing on the use and degradation of agricultural and urban soil were also developed, as well as studies on urban expansion and its consequences for cities and protected areas, with direct application of Change Detection techniques in Portugal, Saudi Arabia and Austria, Mongolia, Pakistan, United States, Brazil and China (Araya, 2009; Dore *et al.,* 2010; Eckert *et al.,* 2015; Ferreira *et al.*, 2015; Usman *et al.,* 2015; Jung and Chang, 2015; Xu *et al.,* 2016; Kleemann *et al.,* 2017; Silveira *et al.,* 2017; Gillespie *et al.,* 2018; Vermote & Kumar, 2019; Viana *et al.,* 2019).

Studies on the history of vegetation cover over three decades are also published, as well as the assessment of greenness, humidity, and senescence conditions, after episodes of fires in Portugal (Baptista *et al.,* 2018; Suess *et al.,* 2018); NDVI trends on land cover and phytoclimatic types in Spain (Novillo *et al.,* 2019) and on the influence of rainfall on vegetation in Portugal (Hill *et al.,* 2008; Costa *et al.,* 2018), proposed to describe the coevolutionary patterns of interactions between man and nature concerning the stages of desertification in the Mediterranean area. Finally, using MODIS NDVI, a population density model of *Anopheles atroparvus*, a species that transmits malaria in Portugal, was built (Lourenço *et al.,* 2011).

In recent years, Change Detection techniques have also been applied to assess the situation and evolution of marshes in different ecological aspects under the anthropogenic influence in different locations around the world. (Sun *et al.,* 2018).

In this context, some works estimated the Net Ecosystem Exchange (NEE), Gross Primary Production (GPP), and Ecosystem Respiration (RECO), based on the NDVI index (Moffett, 2010; Forbrich & Giblin, 2015; Han *et al.,* 2015; Serrano-Ortiz *et al.,* 2015; Bastos *et al.,* 2016; Nahrawi *et al.,* 2017; Lule & Vargas, 2018; Fernandez *et al.,* 2020).

Based on the publication history presented here, it is consistent to state that there is a comprehensive list of applications and purposes of the vegetation indexes concerning environmental issues worldwide. However, there are no records of work carried out with the direct application of Change Detection Techniques in the entire Algarve coast.

Thus, according to the evidence of the relevance of the topic, the preparation of this work was motivated by the possibility that the resulting knowledge can add to the benefit of the scientific community and provide data information for decision-makers to have a better land use management in the region.

2 STATE OF ART

2.1 Integrated Coastal Zone Management (ICZM)

Coastal ecosystems and vital coastal habitats, such as coral reefs, mangroves, and coastal lagoons, are considered the wealthiest and most productive environments on the planet, responsible for providing protein food, economic goods, and services. In these areas, the human population has been overgrowing, and each country must elaborate and constantly update its management and conservation plans to face the decline of natural resources such as freshwater, fertile land, and fishing stocks. In addition, the nations must manage problems related to housing, energy supply, waste, and sewage disposal, among other items of extreme importance. In the coastal zones, the decline of these environmental resources and biodiversity are linked to urban expansion, industrialization, and tourist activities. The effects of these activities are expressed by the more significant amount of solid, liquid, and gaseous wastes, jeopardizing the future of coastal ecosystems and their rich biodiversity (Clark, 2008, MAOTDR, 2007).

To deal with the complexity of coastal management, the development of Integrated Coastal Zone Management (ICZM) strategies for the development and conservation of these areas is essential. ICZM is defined as a dynamic, multidisciplinary, and interactive process to promote sustainable management of coastal zones that covers the entire cycle of information collection, planning, decision making, management, and monitoring of implementation by integration of the terrestrial and marine components of the target territory, in both time and space (Alves *et al.,* 2013, Clark, 2008).

Batista *et al.* (2017) infer that according to conceptual and terminological analysis, several criteria, which will be discussed below, have been used to establish marine and terrestrial boundaries in coastal areas for ICZM planning and land use (LUP). Furthermore, due to the lack of consensus on these concepts and designations regarding the physical, political, economic, and social aspects, Veloso-Gomes *et al.* (2008) proposed a classification of the limits of coastal

zones in Portugal. This classification designated the limits of each zone as follows:

- Littoral (Litoral)— covering the whole Portuguese Economic Exclusive Zone shoreline and all the terrestrial area influenced directly or indirectly by the sea;
- Coastal Zone (Zona Costeira)— the stretch ranging from the 200m depth line to the interior as far as tides, waves, or winds reach and have an influence;
- Coastal Stretch (Orla Costeira)— a stretch of coast that is under the direct influence of sea activity;
- Coastline (Linha de costa)— reference line defined as the intersection between the mean height of sea level and land.

From what has been exposed, it is concluded that the areas of analysis chosen in this work were based on the criteria defined for Littoral areas, where marine and land systems are interdependent, which can be considered as ecotonal zones, term diffused in the ecological sciences, as being transition zones between species or communities, which are used as focal points to detect early changes in the composition of vegetation and other changes due to anthropogenic impact (Brownstein *et al.,* 2015).

2.2 The Natura 2000 network and Ramsar sites

Natura 2000 is a European network for preserving sites of great ecological importance for the breeding of vulnerable species listed under both the Birds Directive and the Habitats Directive. Adopted in 1992, Natura 2000 includes protected nature reserves encompassed in private properties under an appropriate management plan designated by a European Union Member State plan to maintain a favourable conservation status. Such management plans are based on low-intensity agricultural practices (Borre, 2011; Ostermann, 1998).

Many Ramsar sites, discussed below, and other important wetlands are part of the Natura 2000 network. The same is true in the Algarve Region, where

there are Ramsar sites encompassed by NATURA 2000 Zones, such as the Ria Formosa, the Ria de Alvor, and the Marais de Castro Marim.

The Convention on Wetlands constitutes the first of the intergovernmental treaties on the conservation of Bird Habitats, celebrated on February 2, 1971, in Ramsar, Iran. Over the years, the convention has become broader by including protection policies for all ecological aspects of these ecosystems, recognizing such areas as of extreme importance for biodiversity conservation (Bureau, 2001).

The same author defines areas of marsh, or water, whether natural or artificial, permanent or temporary, with water that is static or flowing, fresh, brackish, or salty, including areas of marine water the depth of which at low tide does not exceed six meters, which incorporate riparian and coastal zones adjacent to wetlands as islands or bodies of marine water." The political community widely accepts this definition. However, it receives criticism from the scientific community for being very comprehensive and not being based on biological principles, established by professionals in wildlife biology and botany, the appropriate ones to recognize the values of wetlands.

Ramsar classification is a tool for describing Ramsar sites and aid rapid identification of the main wetland's habitats, providing units for mapping and comparability of concepts and terms in national or regional wetlands inventories. It divides wetlands into three main categories: marine and coastal wetlands, inland wetlands, artificial wetlands, and 40 subdivision types (Mitra *et al.,*2003; Finlayson & van der Valk, 1995).

Wetlands occupy 3% of European territory and 6% of the Earth's surface, representing 15,051,273 ha distributed in 2,247 Ramsar zones. These zones are considered one of the most productive ecosystems on the planet, being comparable to tropical forests and coral reefs, with a wide variety of species of plants, insects, fish, amphibians, reptiles, birds, and mammals (Mitra *et al.,* 2003; Finlayson & van der Valk, 1995).

The values of wetlands are related to human activities that occur within these ecosystems, such as food production, recreation, logging, etc. The total

global value of services provided by coastal areas and wetland ecosystems is estimated at 15.5$ trillion per year, representing about 46% of the total value of services that global ecosystems provide (Finlayson & van der Valk, 1995).

According to Mitra *et al.* (2003), these zones play a complex and vital role in ecology in the region where they are located. Such ecological functions are briefly described in the table below (Table 1).

Table 1: Wetlands: Ecological functions

Function	Description
Water Storage and Ground-Water Recharge	Facilitates water circulation between underground aquifer systems and surface water systems.
Flood control	Absorbs water and minimizes flood flow velocity.
Shoreline stabilization	Stabilize the soil, facilitate sediment deposition and dampen the effects of wave action.
Water quality control	Removal of pollutants from surface water by sediment trapping, nutrient removal, and chemical detoxification.
Climate effects	Return over two-thirds of their annual water inputs to the atmosphere through evapotranspiration.
Community structure and Wildlife Support	Habitat of various animal species; nesting area.

Adapted from Mitra *et al.* (2003).

According to the Ramsar Information Bureau (2001), there are 49 wetlands in Portugal, 31 of which are designated as Wetlands of International Importance (Ramsar Sites), which have an area of 132,487 ha.

The main Natura 2000 sites located in the coastal region of the Algarve are the Ria Formosa (37°03'N 7°47'W) with an area of 23267,48 ha, created by Decree-Law nº 384-B/99 and the south-west Coast (37°28'N 8°88'W), with an area of 100 667,96 ha created by Decree-Law nº. 384-B / 99 and modified by Decree-Law nº 204/2015 (ICNF, 2008).

It is known that many NATURA 2000 sites are also classified as Ramsar Sites. The same occurs in the Algarve Region, where Ramsar sites are also included in NATURA 2000 Zones, such as Ria Formosa, Ria de Alvor, and Sapais de Castro Marim.

2.3 REMOTE SENSING

According to Sabins (2007), Remote Sensing is a method that employs electromagnetic energy such as light, heat, and radio waves, as the means of detecting and measuring a target characteristic, and excludes geophysical methods such as electric, magnetic and gravity surveys that measure force fields.

The electromagnetic radiation (EMR) is the link between the objects of the Earth's surface and the Remote sensors is which according to the understanding of the behaviour of duality, can be considered wave and energy: propagated through empty space, such as sunlight, is, at the same time, a waveform, and a form of energy. Thus, the understanding of the operation of the interactions between EMR and different materials, *e.g.,* rocks, soil, vegetation, water, anthropogenic constructions, is a key requirement for the interpretation of the data collected by the various sensors (Meneses, 2012, Alvarenga *et al.,* 2003; Guedes & Silva, 2018).

Figure 1 demonstrates the Electromagnetic Spectrum with different wavelengths. Where it is possible to observe the visible spectrum, with wavelengths that are between 400μm to 700μm, and represents the segment of the electromagnetic spectrum that the human eye can visualize (NASA, 2010).

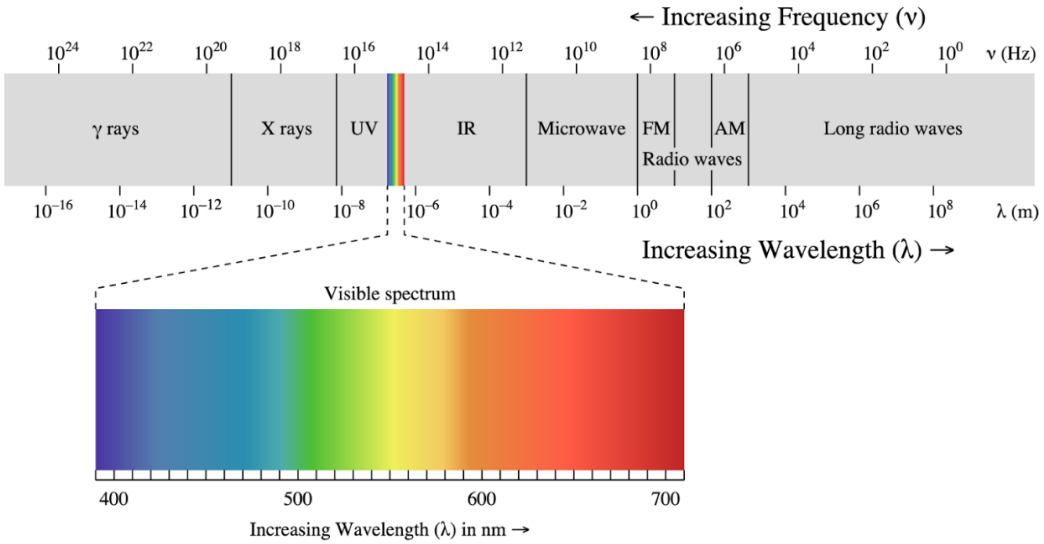

Figure 1: Electromagnetic Spectrum where the visible wavelength is highlighted. (Source: http://spmphysics.onlinetuition.com.my)

Another definition says that Remote Sensing is a science that aims to obtain images of the Earth's surface through the detection and quantitative measurement of the responses of the interactions of electromagnetic radiation with terrestrial materials. This term was created to designate the development of technology and instruments capable of obtaining images of the Earth's surface at Remote distances (Meneses, 2012).

The history of Remote Sensing is directly linked to the invention of the camera, linked to the military service that used it to develop war strategies, by attaching small photographic units to pigeons (Figure 2).

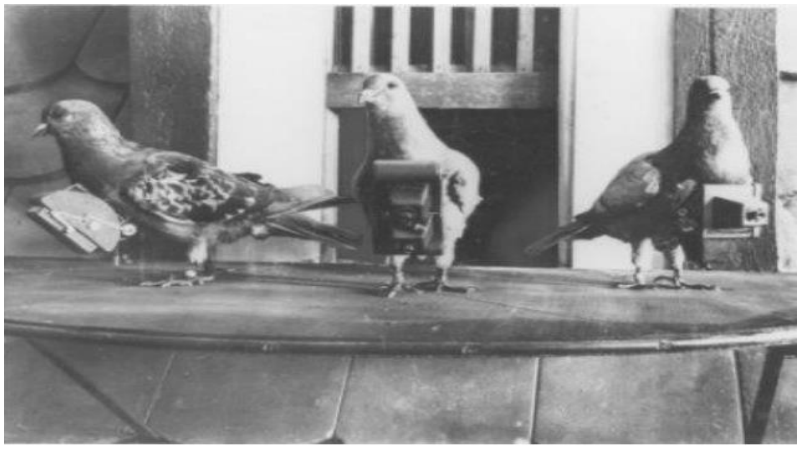

Figure 2: Bavarian pigeon brigade (1903) equipped with cameras to overflight recognition. (Source: adapted from http://sresig.blogspot.com.br/)

Since the launch of the first Earth Resources Technology Satellite in1972 ERTS-1 (Landsat 1) by NASA, has occurred a significant activity related to mapping and monitoring environmental change as a function of anthropogenic pressures and natural processes (Treitz & Rogan, 2004).

Remote sensors can be accoupled in satellites or aircraft and collect information through the Earth's surface's energy, classified as active or passive. Active sensors use internal stimulation to collect data about Earth (i.e., a remote sensing system that emits a beams laser to Earth's surface and measures the time between the signal transmission and reception). The passive sensors record natural energy reflected or emitted from the Earth's surface radiation (Figure 3) (NOAA, 2017).

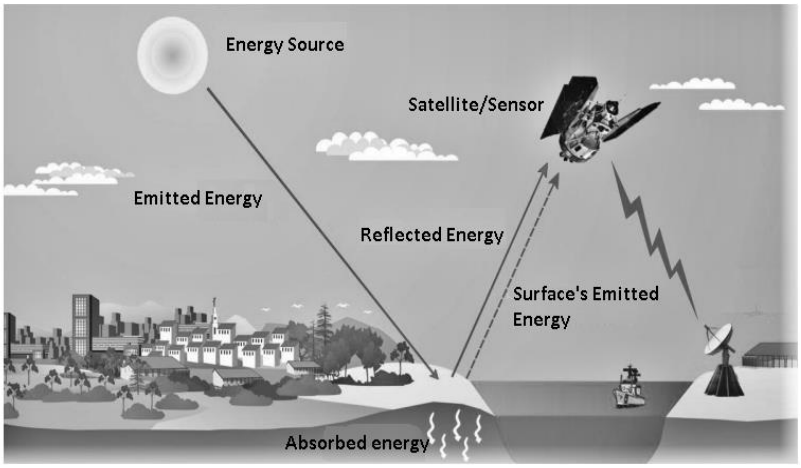

Figure 3: Simplified scheme of passive Remote Sensing.
(Source: adapted from Florenzano, 2002).

Remote Sensing for monitoring continental aquatic systems can be conducted qualitatively or quantitatively. However, the primary demand is for the extraction of quantitative information from parameters that allow both an accurate and detailed description of the trophic state and physical, chemical, and bio-optical processes (Barbosa & Martins, 2019).

Currently, the spectral resolution of the images obtained by the sensors exceeds hundreds of bands, with spatial resolution greater than 1 meter, enabling its applications in the areas of natural resource surveys and thematic mapping, environmental monitoring, detection of natural disasters, forest deforestation, crop forecasts, multi-purpose registration (Table 2) (Meneses, 2012).

Table 2: Main applications of Remote Sensing

.

AREA	DIRECT APPLICATION
Coast	Monitor shoreline changes, track sediment transport and map coastal features. Data can be used for coastal mapping and erosion prevention.
Ocean	Monitor ocean circulation and current systems, measure ocean temperature and wave heights and track sea ice. Data can be used to better understand the oceans and how to best manage ocean resources.
Hazard assessment	Track hurricanes, earthquakes, erosion, and flooding. Data can be used to assess the impacts of a natural disaster and create preparedness strategies to be used before and after hazardous events.
Natural resource management	Monitor land use, map wetlands, and chart wildlife habitats. Data can be used to minimize the damage that urban growth has on the environment and help decide how to best protect natural resources.

Source: Adapted from NASA, 2017.

Track the intensity of earthquakes the trajectory of hurricanes, earthquakes, and floods. The data can assess the impacts of natural disasters and create strategies to be used before and after these events. This has made Remote Sensing one of the most important tools for environmental management. As the demand for more significant amounts and quality of information increases and technology continues to improve, Remote Sensing will become increasingly critical in the future (Rogan & Chen, 2004).

2.4 SATELLITE PROGRAMS REVIEW

2.4.1 The Landsat Program

Since 1972, the Landsat program became indispensable in the acquisition of data to be used in environmental management, both for decision-makers in governments, as well as in the private sector and scientists, by providing essential information for agriculture; monitoring of deforestation and wildfires; natural resources management; urban development; monitoring of water quality and sea surface temperature (Pinto *et al.,*2019).

Landsat 1 was the first Earth-observing satellite to study and monitor landmasses. It carried two instruments: Return Beam Vidicon (RBV) and the Multispectral Scanner (MSS). The RBV was designed to be the main instrument,

but the MSS data were superior. The MSS Sensor recorded data in four bands, two of the infrared, one green, and one red.

The same sensor also equipped the Landsat 2 and Landsat 3. However, Landsat 3 obtained an upgrade in the ground resolution of the RBV sensor, which has now grown to 38m and has two RCA cameras.

In addition to MSS, Landsat 4 and Landsat 5 carried a sensor with improved spectral and spatial resolution, called Thematic Mapper, with seven spectral bands, which were: blue, green, red, near-infrared, medium infrared band one and infrared band two and thermal infrared (Markham & Helder, 2012; Pinto *et al.,* 2019).

Landsat 6 was never operational due to technical problems during launch. As a result, it did not achieve orbit. (Markham *et al.,* 2004).

Landsat 7 was a project developed by NASA, National Oceanic and Atmospheric Administration (NOOA, and the US Geological Survey to obtain high-resolution imagery for environmental monitoring, disaster assessment, land use, regional planning, cartography, range management, oil and mineral exploration.

It carried the Enhanced Thematic Mapper Plus (ETM+) that provided significant spatial resolution improvement, with features such as a panchromatic band with 15m spatial resolution; a panchromatic band with 15m spatial resolution thermal IR channel with 60m spatial resolution, an onboard data recorder. In addition, the Landsat 7 spacecraft provided improved ephemeris and attitude determination. Landsat 7 was considered the best satellite with the highest calibration precision ever acquired until then. Nevertheless, in May 2003, it presented a hardware failure, which caused left wedge-shaped spaces of missing data in the images obtained (Markham *et al.,* 2004).

Landsat 8, launched in February 2013, represents a technological advance, expressed in two different sensors, the Thermal Infrared Sensor (TIRS) and the Operational Land Imager (OLI), collecting data from landmasses, with a resolution of 30 meters in the visible bands, near infrared and shortwave infrared;

15m for the panchromatic band and 100m for the Thermal band. In addition, it has two more bands, compared to the Landsat 7. Band 1 (0.435-0.451 μm), able to collect data from Coast and Aerosol, and band 9 (1.363-1.384 μm) detect clouds composed of ice crystals that often cannot be identified by other bands.

Landsat 8 adds 1.86 million images to the archive, which means nearly 20% of the total archive holdings, and each day Landsat 8 adds another ~700 new scenes (Zanter, 2016; Mazek, 2020). OLI also innovated with the Along-tracking sensor with a four-mirror telescope and 12-bit quantization, which provides better accuracy. In contrast to the Cross-tracking sensors, which equipped all previous versions of the Landsat legacy (Zanter, 2016; Mazek, 2020).

Landsat 9 was launched in September 2021 and joined Landsat 8 in orbit, replacing Landsat 7. With a greater imaging capacity than previous Landsat, more valuable data can be added to Landsat global land archive. The Thermal Infrared Sensor-2 (TIRS-2) is enhanced over Landsat 8 TIRS. Besides, Landsat 9 increased the instrument's life, which now has five years (Mazek,2020; NASA, 2017). Table 3 shows the main characteristics of the Landsat sensors.

Table 3: Specifications of the Landsat sensors

Sensor	**Spectral Bands**	**Spatial Resolution**	**Spectral Region**
MSS	Band 4 (Landsat 1-3): 0.5-0.6 Band 5 (Landsat 1-3): 0.6-0.7 Band 6 (Landsat 1-3): 0.7-0.8 Band 7 (Landsat 1-3): 0.8-1.1 Band 1 (Landsat 4-5): 0.5-0.6 Band 2 (Landsat 4-5): 0.6-0.7 Band 3 (Landsat 4-5): 0.7-0.8 Band 4 (Landsat 4-5): 0.8-1.1	80m 80m	Green Red NIR-1 NIR-2 Green Red NIR-1 NIR-2

Table 3: Specifications of the Landsat sensors (cont.)

Sensor	Spectral Bands	Spatial Resolution	Spectral Region
Thematic Mapper (TM) / Thematic Mapper Plus (TM+)	Band 1 (Landsat 4-5): 0.45-0.52	30m	VNIR
	Band 2 (Landsat 4-5): 0.52-0.60	30m	VNIR
	Band 3 (Landsat 4-5): 0.63-0.69	30m	VNIR
	Band 4 (Landsat 4-5): 0.76-0.90	30m	VNIR
	Band 6 (Landsat 4-510.40.-12.50)	120(30)m	TIR
	Band 7 (Landsat 4-5): 2.08-2.35	30m	SWIR
	Band 8 (Landsat 7): 0.52-.90	15m	Panchromatic
OLI/TIRS	Band 1 (Landsat 8-9) 0.43-0.45	30m	Coastal Aerosol
	Band 2 (Landsat 8-9) 0.45-0.51	30m	Blue
	Band 3 (Landsat 8-9) 0.53-0.59	30m	Green
	Band 4 (Landsat 8-9) 0.64-0.67	30m	Red
	Band 5 (Landsat 8-9) 0.85-0.88	30m	NIR
	Band 6 (Landsat 8-9) 1.57-1.65	30m	SWIR
	Band 7 (Landsat 8-9) 2.11-2.29	30m	SWIR2
	Band 8 (Landsat 8-9) 0.50-0.68	30m	Panchromatic
	Band 9 (Landsat 8-9) 1.36-1.38	30m	Cirrus
	Band 10 (Landsat 8-9) 10.6-11.19	30m	Thermal Infrared (TIRS) 1
	Band 11 (Landsat 8-9) 11.50-12.51	30m	Thermal Infrared (TIRS) 2

Source: adapted from NASA, 2017.

2.4.2 The MODIS Sensor

The Earth Observing System (EOS) is a research program for observing the Earth's surface, oceans, and atmosphere and its interactions funded by NASA. The Earth Science Enterprises (ESE) program has the primary objective of determining the factors which have influenced the global environmental change and its possible consequences for the biosphere, developing an interconnected system used as multi-parameter monitoring (Justice *et al.,* 2002, Anderson *et al.,* 2003).

The ESE launched several satellites, such as TERRA (EO-1) and AQUA (EO-2); however, the description will be focused only on the TERRA satellite for this work. TERRA satellite was launched in December 1999, collecting data available from February 2000. This satellite has five sensors:

- Moderate Resolution Imaging Spectroradiometer (MODIS);
- Multi-angle Imaging Spectroradiometer (MISR);
- Advanced Spaceborne Thermal Emission and Reflection Radiometer (ASTER);
- Clouds and the Earth's Radiant Energy System (CERES);
- Measurement of Pollution in the Troposphere (MOPITT).

These sensors help detect causes, mechanisms, and factors that determine long-term climate variations, in addition to identifying natural hazards and characterizing disasters, and can reduce risks such as fires, volcanism, floods, and droughts. The sensor can also provide data for research focused on land cover, biodiversity, and global primary productivity (Anderson *et al.,* 2003; Middleton *et al.,* 2013).

MODIS is the primary sensor developed for the EOS satellite for researching global climate change. This sensor is characterized by having a broad spatial and spectral coverage and for presenting a continuity in the measurements that are complemented by estimates from other satellites, such as the Advanced Very-High-Resolution Radiometer (AVHRR), used for meteorology and the Coastal Zone Colour Scanner (CZSC) used to monitor

ocean biomass (Justice, 2002). The Table 4 displays some features of the MODIS sensor.

Table 4: MODIS Specifications

Spectral Range	0.4-14.4 µm
Spatial Resolution	250 m (2 bands), 500 m (5 bands), 1000 m (29 bands) in nadir
Repetition coverage	Daily, north of latitude 30º and every other day, for latitudes less than 30º

Source: Adapted from Justice *et al.* (2002).

According to Barker *et al.,* (1992), the MODIS has 36 bands. The first 19 bands are in the region of the electro radiometric spectrum located between 405 nm to 2,155 nm.

Bands 1-7 are intended for terrestrial observations such as Land, Cloud and Aerosols properties; Bands 8-16 to collect ocean data such as Ocean Colour; Phytoplankton and biogeochemistry.

Bands 17-19 for atmospheric water vapour measurements; the Bands 20-36, except for band 26 (1,360-1,390 nm), cover the thermal portion of the spectrum (3,660-1,4385 nm) and are intended for general use within the various scientific branches; Bands 20-23 surface and Cloud Temperature.

Bands 24-25 atmospheric temperature; Bands 26-28 cirrus cloud and water vapour; Band 29 cloud properties; Band 30 ozone; Bands 31-32 surface and cloud Temperature; Bands 33-36 cloud top Altitude.

MODIS generates many products to estimate forest productivity, being, the MOD13, used to calculate vegetation indexes, MOD15 to calculate the Leaf Area Index and Absorbed Photosynthetically Active Radiation (FAPAR), and MOD17 measures Net Primary Production/ Net Photosynthesis accumulated for 8, 32 or 365 days. According Savtchenko *et al.* (2004) and Justice *et al.,* (2002) the MOD17 product, when annual measured, provides an accurate indicator of the growth of terrestrial vegetation and its productivity. This measure allows to define the dynamic flow of carbon of the terrestrial surface in climate modelling.

2.5 - THE LAND COVER AND LAND-USE CHANGE DETECTION TECHNIQUES

The Remote Sensing Change Detection is a technique can be used in a wide range of environmental studies that seek to analyse the progress of land use, as well as land cover changes directly caused by natural forces, or induced by the activities of animals and human, like to for example, the removal of vegetation for purposes of building urban settlements. Timely and accurate change detection of earth's surface provides the foundation for a better understanding of the relationships and interactions between human and natural phenomena to improve the management and use resources. So, it is important to have updated data in real-time to monitor and analyse that changes over time (Asokan & Anitha, 2019).

The digital change detection in Land Cover brought a simpler approach for researchers to process the images, that encompasses measurement of temporal phenomena in multi-date images, purchased by multispectral sensors. Previously it was necessary manage field surveys, which were costly and time-consuming. (Feranec *et al.*,2007; Asokan & Anitha, 2019).

According to Lu *et al.,*2004, good change detection research should answer the following questions: what has changed and what is the rate of this change, discriminate the spatial distribution of changes and evaluate the accuracy of change detection results. To perform a change detection analysis, it is necessary to follow a protocol that includes an image pre-processing, which consists in the geometrical rectification and image registration, the radiometric and atmospheric correction, the topographic correction and selection of suitable technique for change detection analysis.

Several approaches have been developed for land cover (LC) change identification by Remote Sensing data application. However, most authors agree that there is no universal standard technique in Change Detection, which means that there is a great difficulty to end-users in choosing the best approach (Rogan & Chen*, 2004;* Ehlers *et al.,* 2014; Tewkesbury *et al.,* 2015).

However, Lu *et al.* (2004) compiled the main existing techniques, categorizing them into different classes, describing the applicability, pros, and cons of each

one of these techniques: visual analysis, image differencing, image ratioing, transformation, classification; advanced models, Geographical Information Systems (GIS) approaches and other approaches. That said, it should be noted that it is of great importance to know how to choose correctly which algorithm to use in each case of study, since the result, observed in the generated map, can undergo significant changes, obfuscating and distorting the results (Coppin *et al.,* 2004, Tewkesbury *et al.,* 2015).

The integrated GIS/Remote Sensing is one of the most widespread approaches, which is justified by the expansion of computer and software processing capabilities, specifically developed to handle spatially images and data. Due to these unique characteristics, spatial data products have become more widely accepted outside the Remote Sensing community, such as in architecture and civil engineering, in addition to general uses without scientific purposes. The main advantage of using this approach is the ability to bring a larger view of the study area, as it integrates different sources of information that combine the source data with the quantitative data, making the extraction and evaluation of change detection information easier (Asokan & Anitha, 2019).

Direct use of raw spectral data in the analysis of changes makes Change Detection highly susceptible to radiometric variations caused by lighting conditions and seasonality when the images are obtained. Applying the techniques such as regression before the Change Detection allows for attenuating differences in lighting between images

For this work, were used the change detection based on classification from Corinne Land Cover by the European Environment Agency with approaches that integrates the Geographical Information Systems and Remote sensing techniques, as used by the Rahman (2000). This methodology has never been applied to the entire Algarve region, which makes this work innovative.

2.5.1 THE CORINE LAND COVER PROJECT

The Corine programme (coordination of information on the environment) was initiated in the European Union in 1985 taken over by the European Environmental Agency (EEA) as a prototype project working on many different environmental issues (Büttner & Maucha, 2016).

According to Bossard & Otahel (2000), initially, the CORINE Land Cover Program (CLC) applied a method of collecting land cover data based on an inventory of printed copies of satellite images. This was the most reliable approach available in the 1980s.

However, this procedure inevitably introduces errors during digitization, but still reliable today. Nevertheless, the advance of computational processing made possible a higher performance, allowing a cost reduction throughout the inventory process (softcopy).

The CLC database was elaborated visually by interpreting satellite images (SPOT, Landsat TM, and Landsat MSS) and by ancillary data (aerial photographs, topographic or vegetation maps) were used to refine interpretation and the assignment of a territory into one of the CLC classes (Stathopoulou & Keramitsoglou, 2004).

Thus, the CLC has become a valuable tool for assessing the evolution of the LC across the European continent since it is a program in which there is the cooperation of all member states in the production of data essential for the management of the environment (Bossard & Otahel, 2000).

It is presented as a cartographic product, up to a scale of 1:100 000, operationally available for most areas of Europe where it is possible to observe the different subdivisions for the analysed categories (Figure 4).

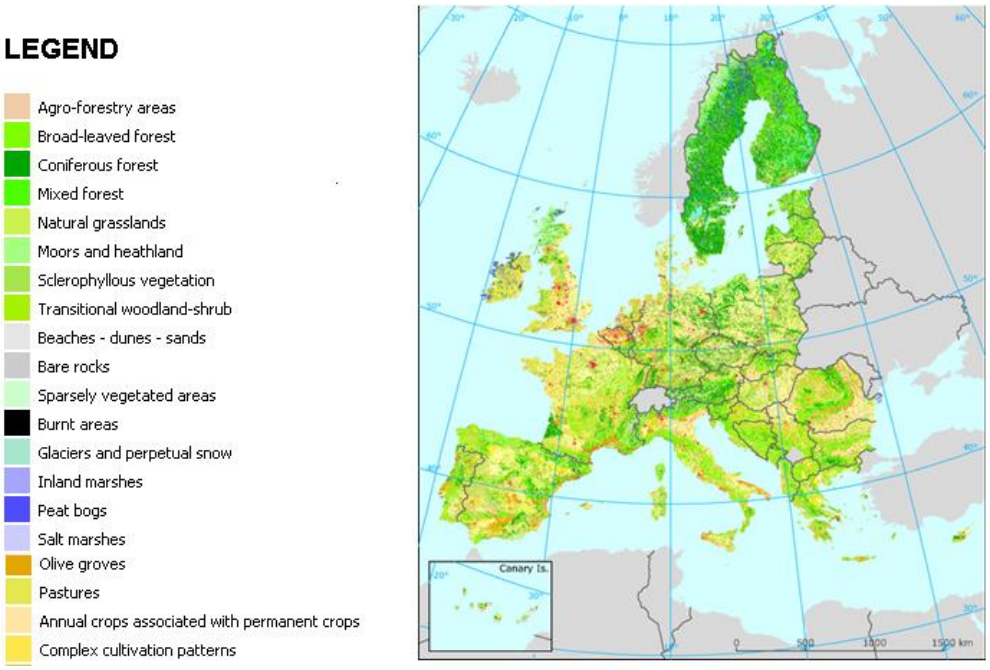

Figure 4: Corine Land Cover mapping subjects examples: https://www.eea.europa.eu/

The first level has 5 classes and corresponds to the main categories of the land cover (forests and semi-natural areas, wetlands, water surfaces, artificial areas, and agricultural land). The second level, with 15 classes, covers physical and physiognomic entities at a higher level of detail and finally level 3 is composed of 44 classes. (Stathopoulou, & Keramitsoglou, 2004; EEA-ETC/TE, 2002). CLC is implemented in 5 – 10 - year periods. This fits with the dynamic of Change of Land Cover observed, which is less than 1% change per year for all countries (Büttner, & Maucha, 2016).

2.6 THE CARBON CYCLE AND GROSS PRIMARY PRODUCTION

Carbon (C) is a solid chemical element at room temperature, with an atomic mass of 12 u, atomic number 6, a member of group 14 of the periodic table. It is non-metal and has tetravalent bonds and three isotopes: ^{12}C and ^{13}C, stable and ^{14}C, in the radioactive form. It is one of the main constituents of all living organisms, being presents from the tissues to the DNA molecules as well as a major component of many minerals. Therefore, along with the geochemical cycles of water, nitrogen, and oxygen, the carbon cycle, plays an essential role in sustaining life on Earth. In this sense, the Earth's biogeochemical cycles

represent a closed system, in which the chemical elements used by the organisms are returned to the system in an altered way, or not, so that they can be recycled and reused, due to the classic law of conservation of masses, which states that: "In nature, nothing is created, nothing is lost. Everything Changes" (Schmidt & Noack, 2000; IPCC, 2013). The carbon cycle is divided into two parts, namely, the geological and biological. In the geological carbon cycle, the diffusion process is responsible for balancing the exchange of carbon dioxide (CO_2) that takes place between the atmosphere and hydrosphere. Moreover, CO_2 dissolves in rainwater to form carbonic acid (H_2CO_3) a solution capable of causing the erosion process in rocks while releasing Ca^{2+} and HCO^{3-} ions. Marine organisms, *e.g.*, molluscs and Porifera, assimilate these ions to form their external structures, such as shells, which accumulate in ocean sediments after the death of these organisms. The cycle will start again with the formation of magma from sediments accumulated, which release O_2 again into the atmosphere by the volcanoes (Schmidt & Noack, 2000, PCC, 2007; Raven, 2013).

The Gross Primary Productivity (GPP) corresponds to plant Photosynthesis, the biological cycle of CO_2 It is the main process of energy transformation in the biosphere, as it is the basis for the transformation of energy used by all food chains and provides oxygen for the breathing of heterotrophic organisms. In general terms, in photosynthesis, light energy is converted into chemical energy and carbon is fixed in organic compounds. In the first stage of the process, light energy will be absorbed by the pigments, which in the case of eukaryotic organisms are chlorophyll and carotenoids, which are concentrated in cellular organelles called chloroplasts. In the second stage, the Calvin cycle uses the energy stored by light-dependent reactions to form glucose and other carbohydrate molecules. Through the Calvin cycle, the carbon found in the atmosphere in the form of carbon dioxide is incorporated into an organic glucose molecule and hence used by the plant itself and by the organisms that feed on it. (Raven, 2013)

2.7 LEAVES ANATOMY AND LIGHT PROCESSING

Vascular plants comprise the largest group of existing plants. Given the many characteristics that distinguish them, the vascular transport system is the main component responsible for its adaptive success (Raven, 2013). The vascular tissues have two major components that occur together and form a continuous vascular system throughout the plant body: xylem, through which water passes upward through the plant body, and phloem, whereby food manufactured in the leaves and other photosynthetic parts of the plant is transported throughout the plant's body, remaining within the root cortex and stem.

The mesophyll is the leaf's ground tissue, with its large volume of intercellular spaces and numerous chloroplasts that are particularly specialized for photosynthesis. The intercellular spaces interact with the atmosphere through the stomata, which facilitate rapid gas exchange, an essential factor in photosynthetic efficiency. The epidermis regulates water vapour, oxygen, and carbon dioxide exchange between the plant and the environment. The guard cells control the closing and opening of the pores of the stomata cells, retaining water inside the tissues. Another function of the epidermis is a waxy coating release, the cuticle, to avoid the loss of water (Raven, 2013). Inside the mesophyll, the interaction of electromagnetic radiation occurs within the visible spectrum trough the photosynthetic pigments such as chlorophylls, xanthophylls, and carotenes present inside the mesophyll (Meneses, 2011). The Figure 5 schematically demonstrates the tissues and cells of the leaves.

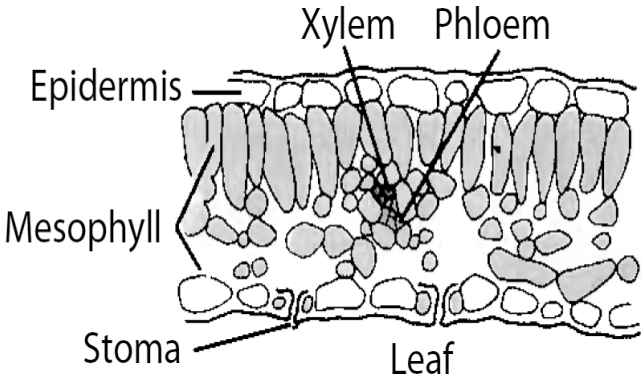

Figure 5: Leaf Internal structure. Source: Raven, (2013).

The interaction between electromagnetic radiation and objects occurs in the ways of reflection, transmission, and absorption, which are dependent on chemical and structural factors such as the presence of photosynthetic pigments, mentioned above, and on the organization of the structures present on the leaf (Ponzoni & Shimabukuru, 2007). The spectral signature of vegetation is given by photosynthetic pigments, most of the electromagnetic energy is absorbed, mainly in the blue (0.45–0.50 μm) and red colour region (0.62–0.75 μm). The absorption in the green region (0.50–0.62 μm) is weak, which is why it is possible to see green vegetation. The reflection in Near-Infrared (NIR) region (0.75-1.30 μm) is very high due the structural of leaves. The existence of water in the leaves will influence the reflectance in the short-wave infrared (SWI) region (1.30-2.50 μm) (Figure 6).

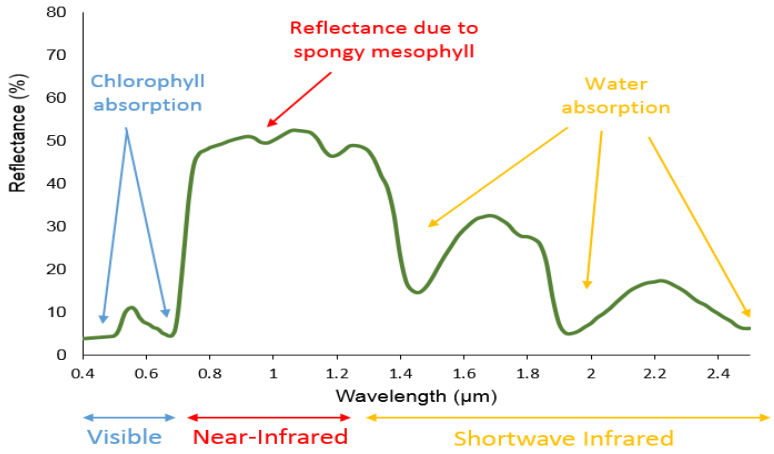

Figure 6: Vegetation has low reflectance in the visible region and high reflectance in the near infrared. (Source: https://gsp.humboldt.edu/OLM/Courses/GSP_216_Online/lesson2-1/vegetation.html)

The near-infrared (NIR) energy can penetrate the mesophyll, due to non-interaction with these pigments, and is refracted in different directions due to the internal air spaces, already mentioned and, consequently, the energy will be released by the lower and upper epidermis (Raven, 2013) (Figure 7).

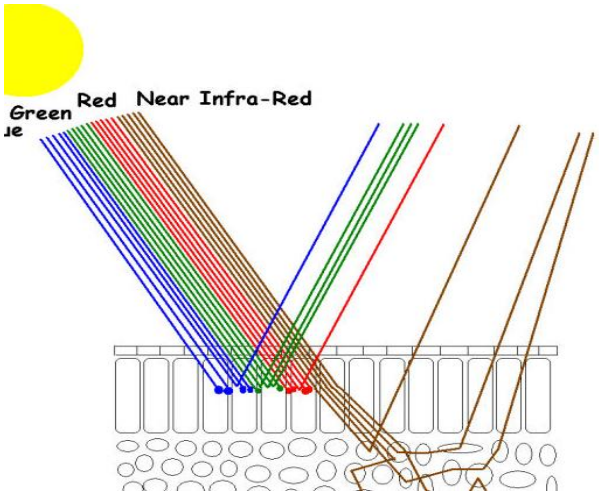

Figure 7: Reflection, refraction and absorption of the distinct wave bands. Source: https://gsp.humboldt.edu/OLM/Courses/GSP_216_Online/lesson2-1/vegetation.html.

Remote Sensing applied to vegetation cover analysis is performed by obtaining and interpreting the electromagnetic waves reflected for the sensors. Information about the vigour and growth of vegetation can provide useful data for many fields of research, such as environmental monitoring and conservation, agriculture, urban landscapes and green roofs (Xue & Su, 2017). The reflectance of vegetation is different in each taxonomic group. For the analysis of the vegetation cover, it is necessary to attend the characteristics of internal leaves and other factors, such as pigmentation, nutritional status, leaf anatomy, phyllotaxis, phenological status, diseases, water content and sun exposure, that can influence the reflectance (Wang *et al.*, 2018). Several vegetation indexes based on the visible and NIR reflectance were developed to analyse the vegetation cover.

2.8 VEGETATION INDEXES

Vegetation indexes are extensively used to evaluate the growth and vigour of plants that can be related to water content, pigments, sugar and carbohydrate content, protein, and aromatics content, among others (Xue & Su, 2017).

2.8.1 The normalized difference Index

The Normalized Difference Vegetation Index (NDVI), is an important indicator used in the detection of changes in vegetation cover for different periods in the same area. The main objective of NDVI is to improve the analysis of vegetation information with Remote Sensing data. It has been used to calculate canopy factors such as biomass, leaf area index (LAI), absorbed photosynthetically active radiation (APAR) and canopy photosynthetic capacity. For reasons related to its simplicity, its long history, and its reliance on easily obtained multispectral bands, it has led NDVI to become the most popular index used for evaluating vegetation. Its usefulness ability to quickly outline vegetative stress represented a major advance in all Remote Sensing data carried out by observation satellites, which are equipped to produce this index in different spatial and temporal resolutions (Huang *et al.,*2020). The index was developed by Rouse (1974) based on the fact that chlorophyll absorbs RED and the structure of the mesophyll leaf spreads the NIR.

2.8.2 The photochemical reflectance index

The use of vegetation indices that use specific wavelengths that affect photosynthetic pigments such as chlorophyll, which are affected by conditions of water stress, has become widespread, and one of the most used for these purposes is the Photochemical Reflectance Index (PRI) (Gamon *et al*, 1992; Xue & Su, 2017). Although, in contrast to NDVI, which uses NIR to detect water stress in plants, the PRI has been used as a water stress indicator based on visible spectral bands (Gamon *et al*, 1992). The PRI index is analogous to that of NDVI and uses green and blue reflectance (Rahman *et al.,*2000). Nevertheless, NDVI is not sufficient to capture dynamic physiological processes that can occur, *e.g*., in drought-tolerant species that seasonally adapt the efficiency of light usage and photosynthetic activity, which can be completely reduced (Xue & Su, 2017).

According to Gamon *et al.* (1992), the PRI is a reliable method for assessing ecophysiological variables related to photosynthetic efficiency at leaf levels in a varied number of species on time scales. Furthermore, provide information about the status of plant nutrients to indicate the total concentration of chlorophyll and

the relationship between carotenoids and chlorophyll to detect long-term stress effects.

2.8.3 The carbon dioxide flow index

The greenhouse effect and global warming, which cause climate change throughout the planet, occur because of the high concentration of gases such as carbon dioxide (CO_2), methane (CH_4) and nitrous oxide (N_2O), from anthropic actions (IPCC, 2007; INPE, 2012).

Atmospheric concentrations of CO_2, considered the main cause of the alterations in ecosystems, are responding to climate change in a proportional and direct order, which has negatively impacted primary productivity and soil carbon stocks. There is an increasing demand for research focused on the stock and sequestration of CO_2, carried out by forest environments, marshes and even the oceans (Almeida & Rocha, 2018). Regarding this, by storing carbon, vegetation helps to minimize the effects of the impact of carbon dioxide (CO_2) on the environment, in addition to being fundamental in the process of photosynthesis (Folharini & Oliveira, 2017). According to Rahman *et al.* (2001), the flow of carbon (CO_2flux) on the planet can be accounted for through the interaction of NDVI and PRI.

3 OBJECTIVES

The main objective of this study was to carry out an assessment, through Remote Sensing and GIS techniques, on the evolution of plant biomass, correlating with the production of CO_2 and to evaluate the evolution of land use and occupation, in the coastal zone of Algarve, Portugal.

As a specific objective, a digital cartographic collection of specific vegetation indices and land use was made between the years 1990 to 2020.

To achieve these objectives several steps were conducted:

- Determination and mapping of the Vegetation indexes, namely, NDVI, PRI, and CO_2flux in a time series of Landsat images from 1990 to 2020;
- Correlation of the CO_2flux with MODIS GPP products from 2000 to 2020;
- Calculation and mapping of land Cover Change detection based on the Copernicus Corine Land Cover program in a time series from 1990 to 2018.

4 METHODOLOGY

4.1 STUDY AREA

The Algarve region is located in the southern of continental Portugal, representing 5.5% of the national territory, which corresponds to a total area of 4,899 km^2 (Vaz, 2011).

According to Oliveira (2013), the Köppen-Geiger classification system characterizes the region as a hot-summer Mediterranean climate (Csa). The main climate characteristics for the region in the period 1971-2000 are: (i) the accumulated annual average of precipitation in the Algarve region, is 594.2 mm with 789.8 mm, for the maximum and 433.7 mm for the minimum; (ii) precipitation is distributed between September and May, with a greater concentration, 88%, between October and April; (iii) the dry period is concentrated in the months of June to August; (iv) the annual mean of the temperature ranged between 15.4 ºC and 16.4 ºC, the annual mean of the minimum air temperature ranged between 10.7°C and 11,7 °C and the annual mean of the maximum air temperature ranged between 20.1 °C and 21.2 °C; (v) the average relative humidity of the air varies between 69% and 71%; (vi) the insolation accounted for in the measurement of global solar radiation ranged between 169 W/m^2 and 177 W/m^2; and (vii) the potential evapotranspiration varies between 3.5 mm/day and 3.6 mm/day (CLIMA, 2022).

However, the morphology allows the formation of microclimates, which establish, as said before, unique conditions for the presence of important and complex coastal saltwater lagoons and barrier islands (Andrade & Santos, 2021).

For this work, a buffer of 7 km from the coastline was defined under the EPSG 32629 WGS 84 /UTM 49 coordinate reference system, to cover the main urban centres and Ramsar/Natura 2000 sites, areas influenced directly or indirectly by the sea (Figure 8).

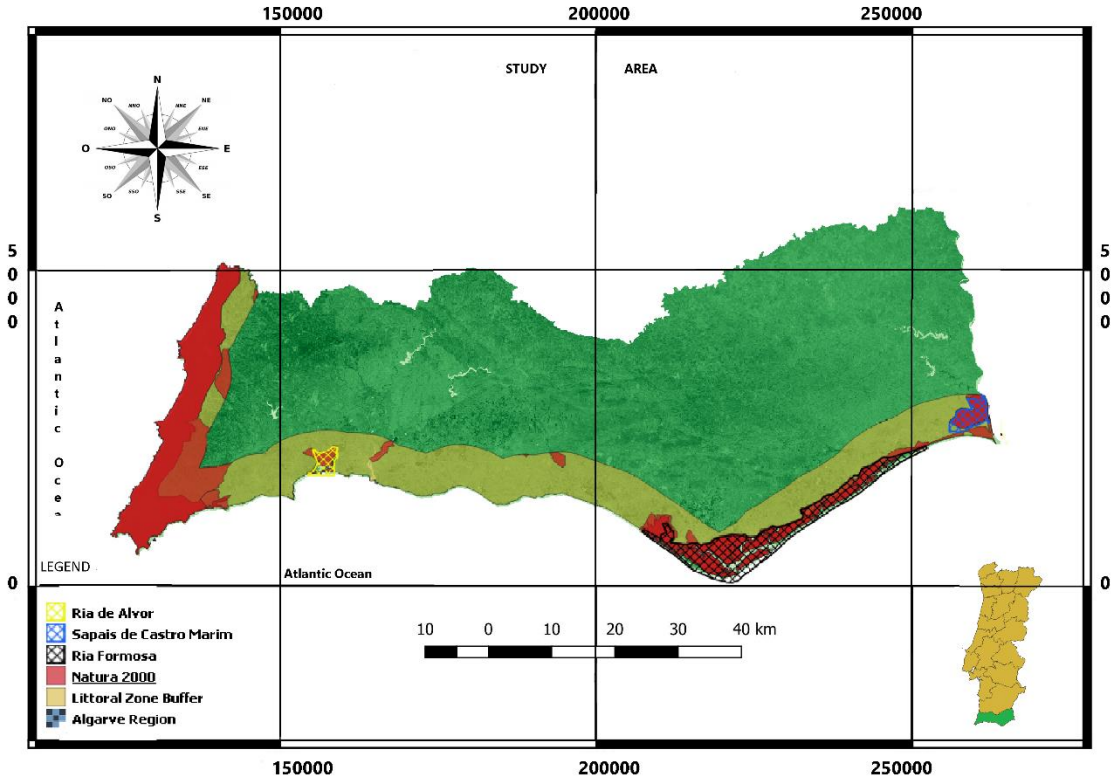

Figure 8: Study Area highlighted by the buffer in Algarve's Coastal Zone, encompassing the Natura 2000 and RAMSAR sites at 1: 600 scale (Source: Elaborated by the Author).

The Ria Formosa is classified as a Natural Park (law-Decree 373/87, 9th December), due to its great biodiversity and habitat variety, it is the most important wetland of Portugal is also protected under the Ramsar Convention, Ramsar site n° 212, and is part of the EU Natura 2000 network of protected areas (Aníbal *et al.,* 2019). The Ria Formosa is a complex of coastal saltwater lagoons and barrier islands with vast lakes, shoals, and dune systems, supporting various anthropogenic activities, including tourism, aquaculture and fisheries (Kombiadou *et al.,* 2019). This area (16,000 ha), with a vegetation cover composed mainly of halophytic and psamophilic species, is home to numerous species of breeding, wintering, and staging waterbirds. It is worth mentioning that in these regions, most of the urban centres of the Algarve region are located, represented by the cities of Faro, Olhão and Tavira (Costa *et al.,*1996, Vaz, 2011). The Ria Formosa has a barrier island system of approximately 50 km in length, consisting of five islands (Barreta, Culatra, Armona, Tavira and Cabanas) and two peninsulas (Ancão and Cacela), with dune strips of widths between 100 and 750 m. These barrier islands enable the sedimentary, water and nutrient exchanges between

the lagoon environment and the ocean (Costa *et al.,*1996; Marcelo & Fonseca, 1998, Aníbal *et al.,* 2019).

The Sapais de Castro Marim encompass a Nature Reserve under national legislation and was subsequently declared a Special Protection Area of the EC Wild Birds Directive, Ramsar site n° 829; is one of the most important wetlands in the country, as it presents an enormous wealth and diversity of fauna and flora species, which is composed of halophytic communities and low shrubby (Sá, 2012; ICNF, 2008). It is a complex of alluvial plains located in the Eastern Algarve, near the mouth of the Guadiana River, with 2,235 ha, of shallow waters with a range of salinities strongly influenced by the balance between freshwater inputs, penetration of saltwater from the ocean and evaporation, attenuating occasional floods and retain freshwater from the Guadiana River to one of the driest areas in Portugal. Commercial salt production has furthered the change of land use over the years (Susano & Goncalves, 2020; Sá, 2012; ICNF, 2008. Moura *et al.,* 2017).

The Ria de Alvor is a Protected Landscape Area, a National Ecological Reserve, Ramsar site n° 827. A coastal lagoon and estuarine wetland system separated from the sea by sand spits with 1,454 ha. The site includes stable and mobile dunes with characteristic vegetation, mudflats, tidal salt marshes, and salt pans - an important stopover site for many trans-Saharan birds.

The area is most valued for its aquatic life, which includes important commercial shellfish production. This site is part of urban-tourism contexts, marked by seasonality in tourism demand, and within a very consolidated residential area (ICNF, 2008; de Almeida, 2016).

The vegetational formation of the Ramsar sites in the Algarve region is composed of halophytic and psamophilic species. Halophytic are known for their ability to adapt to life in saline environments (Moghaieb & Fujita, 2004). Psamophilic vegetation presents well-demarcated segregation, which is strictly linked to a geomorphological zonation, reflected in embryonic, primary, and semi-

stabilized dunes. (Costa & Espírito-Santo, 1996; Liu *et al.,*2016). The figure 9 displays examples of species representing the respective groups.

Figure 9: A - *Spergularia-bocconei.* B- *Cactus sp.* Species representing the halophytic (A) and psamophilic (B) groups. (Source: https://live.staticflickr.com/)

4.2 DATA ACQUISITION AND TREATMENT

For the manipulation and geoprocessing of GIS data and Remote Sensing, the software Qgis 3.20 and ArcGis 10.3 were used for it.

The GIS shapefiles files used, referring to the cartography of the Portuguese territory, the environmental protection areas, the Natura 2000 Network and the Ramsar Sites were respectively downloaded from the QGIS HCMGIS plugin and from the websites, https://rsis.ramsar.org/ris/ and https://ec.europa.eu/.

4.2.1 LANDSAT IMAGERY ACQUISITION

The necessary data to be used in this work was obtained from the United States Geological Survey website GloVis (usgs.gov), a public accessible database, where it is possible to acquire images of the Landsat satellites (Figure 10).

For this work, all Landsat images used were captured during the summer season since 1990. This time of year, was chosen due to the low rainfall recorded for the region over the decades, thus favouring more reliable results, as it reveals the state of the vegetation and GPP rates under more severe conditions.

Figure 10: Landsat image of study area in Glovis webpage.
(Source: https://glovis.usgs.gov/app).

Thus, when applying criteria such as less than 10% of Land Cloud Covering it was noted that many images did not meet the standards, in addition to also not displaying the entire study area. What caused the sample supply to be reduced. The images belong to LEVEL-1, which means that they do not have any type of atmospheric correction, whereby was made subsequently. All images were acquired and then the QGIS software was used to project them to the WGS84 coordinate system.

4.3 LANDSAT IMAGERY PRE-SELECTION

According to Moffet (2010), it becomes difficult to carry out this type of study, with the application of vegetation indexes, due to the variation of the tide, which floods a good portion of the land that emerges in the period of low water level, affecting the results, when compared at different times. The same author affirms that the surface energy balance of the unflooded salt marsh is similar to a sparse crop, with the soil and canopy being responsible for large portions of

energy, water and carbon exchange, and, during the flood period, the energy balance resembled that of a well-irrigated grass reference crop. The same author affirms that the degree flood affects energy, water and carbon exchanges between the different humid zones and the atmosphere and is directly correlated with the depth and duration of the high tide.

For this reason, only images were selected in which the tide was at a low level, to avoid possible distortions imposed on the results when calculating the vegetation indices along in the time series.

For this, the metadata file supplied with the Level-1 products of each Landsat image was accessed, to obtain the day and time of capture, and then the Wtides software (Figure 11) was used, where it was possible to observe the tide table for each date, time and a specific port. For the Sapais de Castro Marim, tidal data from the Port of Vila Real of Santo António were collected. For the Ria Formosa, the data from the Faro-Olhão port were extracted and, finally, for the Ria de Alvor, the tide data from the Port of Lagos was used.

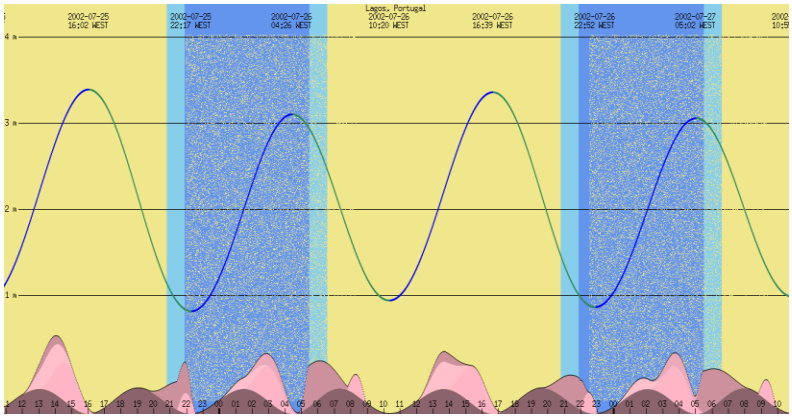

Figure 11: Software Wtides displaying the Tide variation from the port of Lagos, Portugal in 2002-07-25.

According to Faracini (2017), the results obtained by the Wtides software were compared with the tide table of the Hydrographic Institute of the Navy of Portugal, with a margin of error of approximately 2 centimetres. And, for convenience purposes, it was chosen to select images with a time spacing between 5 and 7 years, to save computational data processing time, and so that the differences between the resulting values between these periods were more

prominent. Table 5 shows the tide level for the day and time of the year in which the Landsat images were obtained for each port.

Table 5: Tide Level for each specific port

DATE	Satellite /Sensor	HOUR	Ria Formosa	Castro Marim	Ria de Alvor
1990/08/17	LANDSAT 5/TM	10:28 A.M.	1.13	0.98	1.07
1997/08/20	LANDSAT 5/TM	10:40 A.M.	0.53	0.47	0.46
2002/07/25	LANDSAT 5/TM	10:56 A.M.	1.01	1.02	1.06
2007/08/16	LANDSAT 5/TM	11:02 A.M.	0.96	1.01	0.95
2010/08/24	LANDSAT 5/M	10:57 A.M.	1.27	1.33	1.43
2015/07/21	LANDSAT 8/OLI	11:08 A.M.	1.37	1.38	1.29
2020/08/21	LANDSAT 8/OLI	11:08 A.M.	1.12	1.11	1.26

4.4 LANDSAT DATA IMAGERY CALIBRATION

The energy emitted or reflected by the Earth's surface, captured and measured by sensors of satellites, can be distorted by the interaction of atmospheric factors and the sun. Therefore, the corrections and radiometric calibration applied to the pixel values are essential before using time-series image data. From this premise, after acquiring the images, it was necessary (to convert the original format of the pixels, which are primarily presented in Digital Levels (DN) and convert into values that express the reflectance (ρ_λ) (Gaida *et al.*, 2020). The conversion of the Digital Levels into reflectance of the Landsat satellites is given by equation 1:

$$\rho_\lambda' = M_\rho \times Q_{calc} + A_\rho \quad (1)$$

Where, ρ_λ' is the TOA planetary reflectance without correction for solar angle, M_ρ is band-specific multiplicative rescaling factor from the metadata, $Qcal$

is the quantized and calibrated and standard product pixel values (DN) and A_ρ is the Band specific additive rescaling from the metadata.

But According to Zanter (2016), the ρλ does not correspond to the true reflectance TOA, as it does not take into account the correction of the solar elevation angle, which is not present in Landsat's Level 1 products, instead, the scene-centre solar elevation angle in the metadata is used. However, there is a possibility to calculate the per-pixel solar elevation angle across the entire scene.

After choosing the solar elevation angle, it is possible to convert to TOA Reflectance using equation 2:

$$\rho_\lambda = \frac{\rho_\lambda'}{\cos(\theta_{SZ})} = \frac{\rho_\lambda'}{\text{sen}(\theta_{SE})} \quad (2)$$

Where θ_{SZ} is the local solar zenith angle ($\theta_{SZ} = 90^o - \theta_{SE}$) and θ_{SE} is the local sun elevation in degrees. Figure 12 displays the same image before and after the corrections mentioned.

Figure 12: The image on the right is presented without the necessary atmospheric corrections. The image on the right is already calibrated (Source: NOOA, 2017).

4.5 Vegetation Indexes Calculation

From the corrections and calibration of the images, the Normalized Difference Vegetation Index (NDVI), proposed by Rouse *et al.* (1974) was calculated, which aims to enhance the vegetation cover through the reflected (NIR) and absorbed (RED) energy, representing the vigour of the vegetation cover, being calculated using the equation given below:

$$NDVI = \frac{\rho_{NIR} - \rho_{RED}}{\rho_{NIR} + \rho_{RED}} \quad (3)$$

Where the ρ_{NIR} represents the reflectance of the band in the infrared and the ρ_{RED} represents the reflectance of the red band. The NDVI values range from -1 (no vegetation) to 1(maximum vegetation cover). The common range for green vegetation is 0.2-0.8. Values next to zero represent bare soil (Pedras *et al.,*2014).

The reclassification of NDVI values was made based on da Rocha Almeida & da Silva Rocha (2018), so that it was displayed in 4 classes, with values between 1 and 5 (Table 6).

Table 6 NDVI: Reclass and designation in four distinct classes

Class	**Range**	**Definition**
1	-0.1 thru 0.1	No Vegetation/ Water
2	0.1 thru 0.25	Sparse Vegetation
3	0.25 thru 0.45	Moderate Vegetation
4	0.45 thru 1	Dense Vegetation

Gamon *et al.,* (1992), proposed the Photochemical Reflectance Index (PRI), an index of instant efficiency factor of Ecosystem Photosynthetic Rates, which measures vegetation light-use efficiency, through the relationship between the spectral bands of Blue and Green, given equation 4:

$$PRI = \frac{\rho_{BLUE} - \rho_{GREEN}}{\rho_{BLUE} + \rho_{GREEN}} \quad (4)$$

Where ρ_{BLUE} is the reflectance for the blue band the ρ_{GREEN} is the reflectance for the green band. Values range between -1 and 1, where the range between -0.2 and 0.2 represents healthy vegetation (Gamon *et al.*, 1997).

After obtaining *PRI*, was rescheduled, following Rahman *et al.* (2000) and the *sPRI* is obtained by equation 5. The *sPRI* is in the range of 0 to 1.

$$sPRI = \frac{PRI+1}{2} \quad (5)$$

The images were clipped so that only data from the Algarve Littoral were represented.

4.6 THE CO_2*FLUX* AND GPP CALCULATION

Following, the CO_2flux index was calculated and indicates the efficiency of the carbon capture process by the vegetation (Equation 6).

$$CO_{2flux} = NDVI \times sPRI \quad (6)$$

The average of carbon sequestration was determined based on GPP data provided by AQUA/MODIS images for eight days with a resolution of 500 m, measured in KgC / m^2 × 0.0001 (Table 7).

Table 7: MODIS Products List selection

Nº	Product fileName	Year	Month	Cumulative days
1	MYD17A2H.A2002209.h17v05.006.2015149145727	2002	August	6-13
2	MYD17A2H.A2007225.h17v05.006.2015165003357	2007	August	22-29
4	MYD17A2H.A2010233.h17v05.006.2015211092439	2010	August	14-21
5	MYD17A2H.A2015201.h17v05.006.2015304053348	2015	August	13-20
6	MYD17A2H.A2020161.h17v05.006.2020170065304	2020	August	14-21

The images are originally available in Hierarchical Data Format (HDF) format, being converted to TIFF format (tagged image file format). Then was used QGIS to apply the clipping tool to the study area. A conversion from Raster to vector was performed, using the geoprocessing tools, due to the different spatial resolutions between the CO_2flux maps (30 m) and the spatial resolution of the GPP map where each polygon corresponds to the delimitation of each pixel (500m). It was created tables for the different maps with the averages of the variables of GPP and CO_2flux. The average of the GPP is equivalent to the value of each pixel of the GPP map and the average of the CO_2flux was calculated from the average of the set of pixels that intersect each grid of the shapefile of the study area (Fernandez *et al.,* 2021).

Linear regression was established, from the GPP values (response variable) and the mean values of CO_2flux (explanatory variable) for different epochs. The assess the goodness-of-fit was do it by R-squared (R^2) value analysis. To acquire the graphical results of these regressions, the Zonal Statistics tool of the Qgis Software was used, which related the average values for each pixel of the CO_2flux index with the values of the GPP images. However, before that, for the calculation to be possible, it was necessary to vectorize the Raster files of the GPP files, which once underwent the first conversion from HDF to Raster.

Once this was done, the resulting vector files were converted to CSV. format, where the scatter plots were generated.

4.7 Acquisition and Processing of Corine land cover data

The Corine Land Cover data, previously described, was downloaded from the website https://land.copernicus.eu/pan-european/corine-land-cover.

The entire time series available was used, being: CLC1990, CLC2000, CLC2006, CLC2012 and CLC 2018.

The data were pre-processed, with the application of geoprocessing tools to cut the original file, in which there is a representation of all the countries of the European Union, so that only the data relating to the Algarve region were

presented, and then, a buffer of 10,000 m was applied, that represents the coastal zone (Figure 8), so that only the data from that territorial range were considered in the analysis.

The Corine Land cover has in its originality, several subdivisions of 5 main designations, which are grouped in a numerical variation, in its table of attributes. To facilitate the analysis and have a better cartographic demonstration for this study, the file was reclassified, so that all subclassifications present in the original format were diluted into 5 main classes, using the “aggregate” geoprocessing tool in QGIS. Table 8 shows the results of this classification.

Table 8: Corine Land Cover Reclass

Range	Designation
100 thru 199	Industrial/ Urban Zones
200 thru 299	Farming Zones
300 thru 399	Vegetation Zones
400 thru 499	Wetlands Zones
499 thru 500	Water Bodies

Subsequently, the reclassification, the area and percentage of each index corresponding to each category, was calculated from the manipulation of the attributes table of the Corinne Land cover shapefile file, and the use of other geoprocessing tools available from QGIS.

5 RESULTS

5.1 NDVI

Table 9, shows the NDVI values between 1990 and 2020 obtained from Landsat 5's TM sensor and Landsat 8 OLI sensor. With the TM sensor, the years that showed greatest the NDVI range were 1990 and 2010. In 1997, 2002 and 2007, the NDVI range is less because the negative values are closer to 0 when compared to other years. It is possible to observe that the years 2007 and 2010 show higher standard deviations of the NDVI. In OLI sensor images had the highest NDVI difference values happened in 2020.

Table 9: NDVI and Std deviation Values

Year	Satellite/Sensor	NDVI Values	Mean	Std. Deviation
1990	Landsat 5/TM	-0.79 – 0.78	0.02	0.41
1997	Landsat 5/TM	-0.59 – 0.76	0.09	0.43
2002	Landsat 5/TM	-0.56 – 0.73	0.09	0.40
2007	Landsat 5/TM	-0.58 – 0.75	0.09	0.58
2010	Landsat 5/TM	-0.76 – 0.80	0.02	0.58
2015	Landsat 8/OLI	-0.69 – 0.83	0.07	0.43
2020	Landsat 8/OLI	-0.79 –0.82	0.02	0.62

To better understand the NDVI difference, the values were reclassified in four classes and calculated the percentage of each occupation class (Table 10 and Figure 13).

Table 10: NDVI Reclassification Percentage

Vegetation Class	1990 Landsat 5 TM	1997 Landsat 5 TM	2002 Landsat 5 TM	2007 Landsat 5 TM	2010 Landsat 5 TM	2015 Landsat 8 OLI	2020 Landsat 8 OLI
No Vegetation/Water	7.6%	3.7%	4.3%	4.3%	6.2%	2.8%	3.4%
Sparse	48.0%	50.5%	43.0%	45.7%	39.1%	21.8%	27.4%
Moderate	39.0%	41.8%	46.3%	42.7%	43.7%	58.4%	54.7%
Dense	5.4%	4.0%	6.4%	7.3%	11.0%	17.0%	14.5%

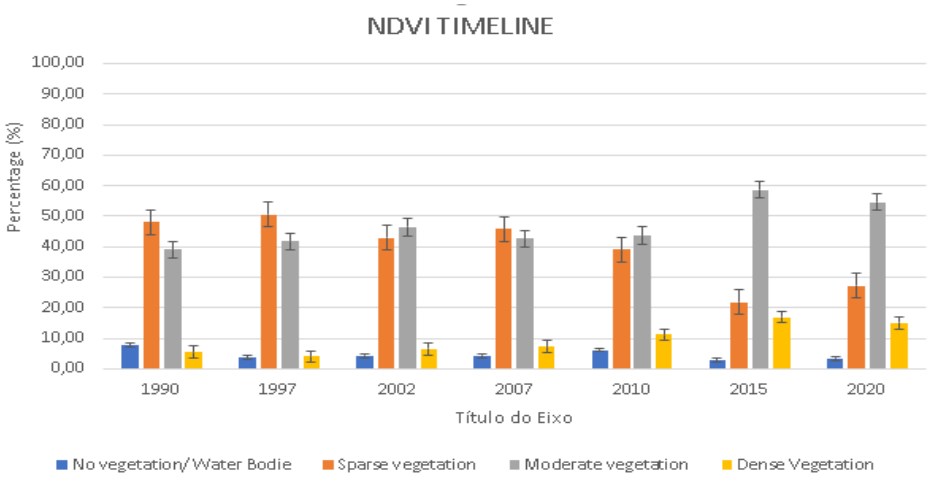

Figure 13: Percentage of the NDVI vegetation classes for the period of study (Source: Elaborated by the Author).

By analyzing Table 10, it is possible to observe the following characteristics:

Class 1 represents no vegetation or water. For images collected by the TM sensor, in 1990, this class had 7.6% of the occupation. After this year until 2007 occurred a decrease to half of the area. In 2010 happened an increase to 6.2%. For images of the 2015 and 2020, acquired by the OLI sensor, the areas for this class decrease to around 3%.

Class 2 represents sparse vegetation. The TM images acquired in 2007 showed that this class ranged between 43.0% to 50.5% area. In 2010 occurred a decrease to 39.1%. In 2015 and 2020, with OLI sensor had a considerable drop, never reaching 30% area (21.8% and 27.4%, respectively).

Class 3 represents Moderate vegetation. In period 1990 -2010 this class had an occupation around 40% reaching the maximum in 2002 (46.3%). In 2015 and 2020, with sensor OLI, this class presents the highest values between 58.4% and 54.7%, respectively.

Class 4 represents Dense Vegetation. In 1990-2010 the occupation rates ranged from between the minimum value of 4.0% (1997) and maximum value of 11.0% (2010). For the results of the OLI sensor, the class reached a percentage of 17.0% in 2015 and 14.5% in 2020. Figures 14-20 show the NDVIs mapping results for each date studied.

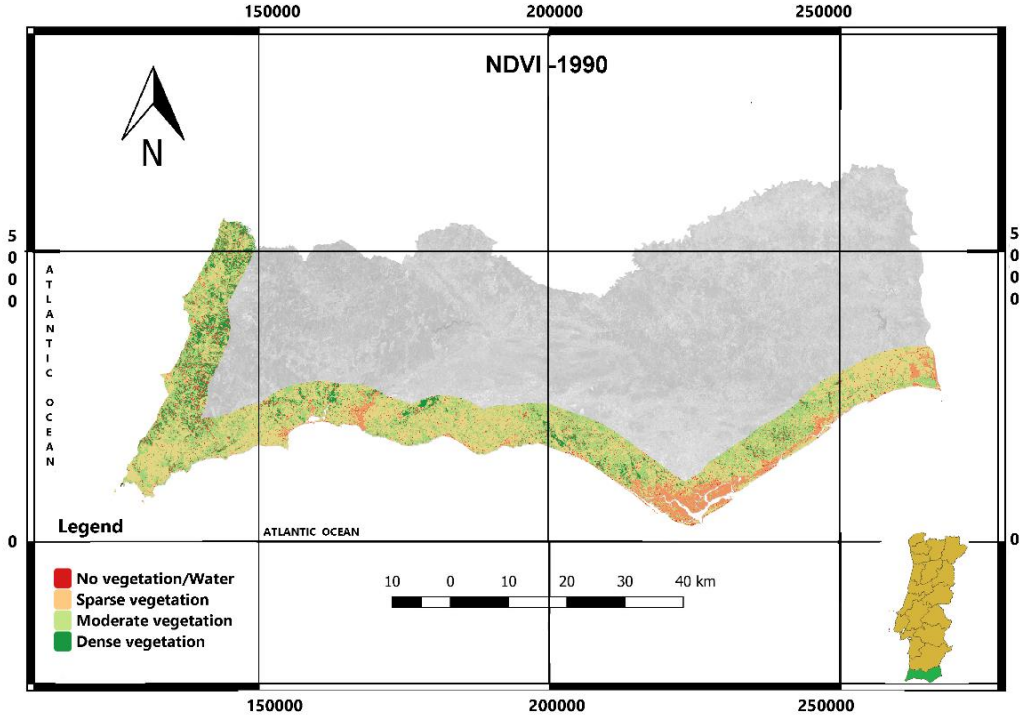

Figure 14: NDVI map from Coastal Algarve in 1990 (Source: Elaborated by the Author)

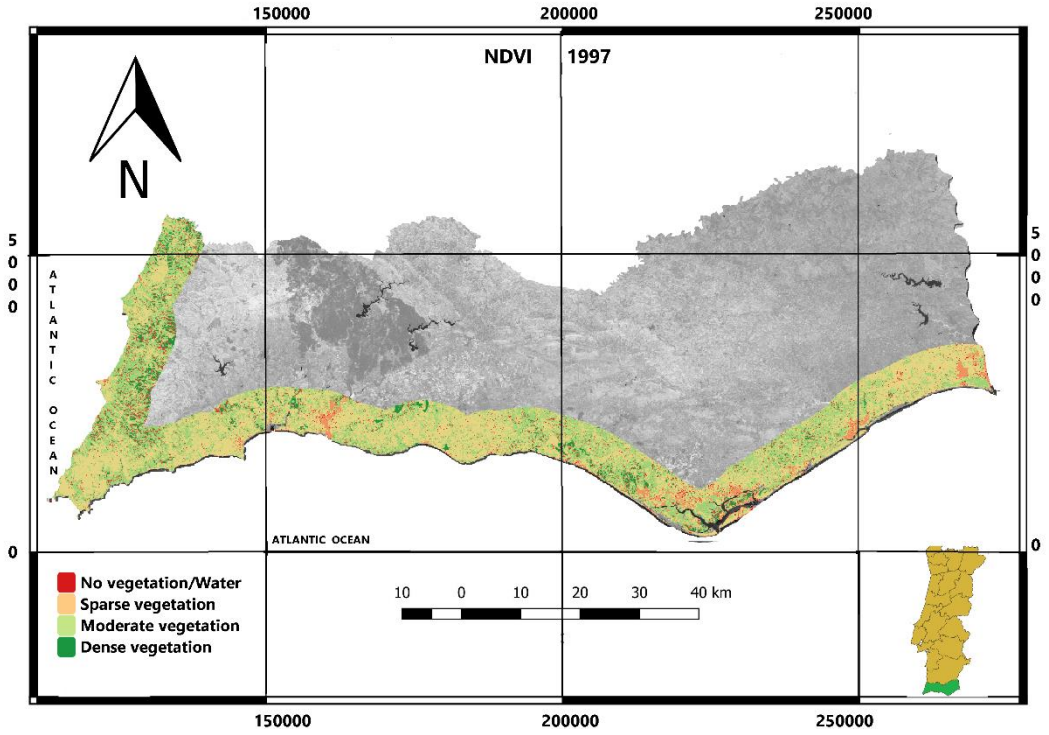

Figure 15: NDVI map from Algarve Coast in 1997 (Source: Elaborated by the Author).

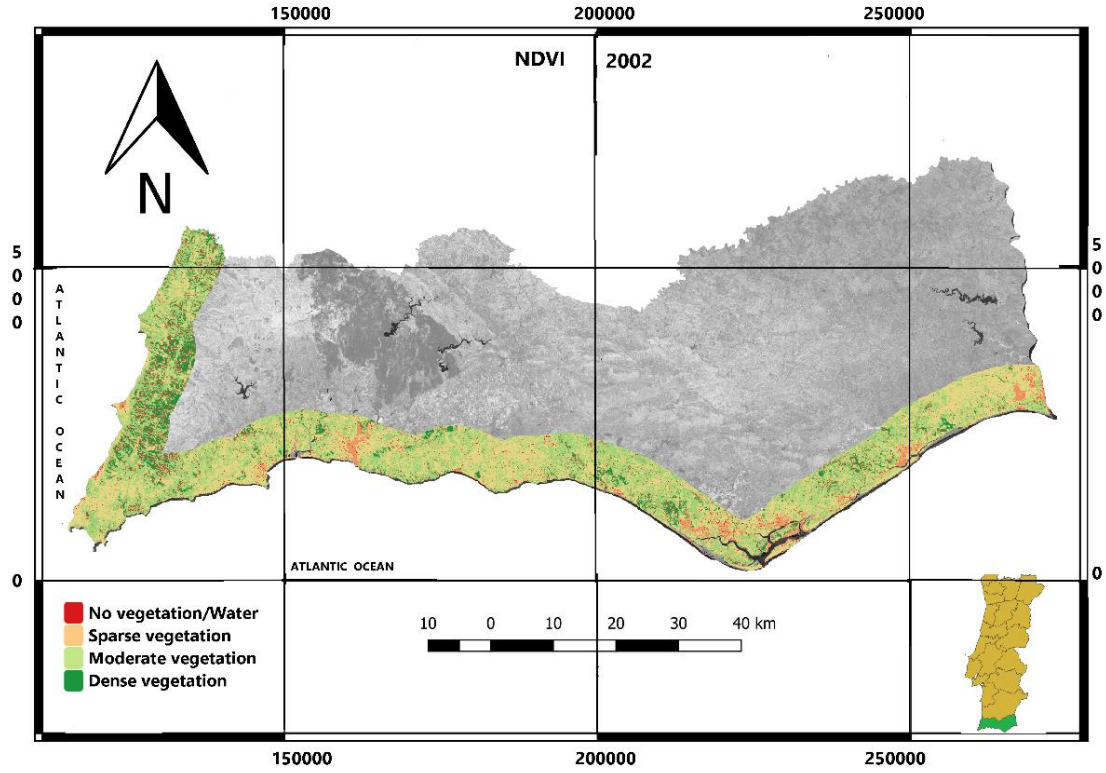

Figure 16: NDVI map from Algarve Coast in 2002 (Source: elaborated by the Author).

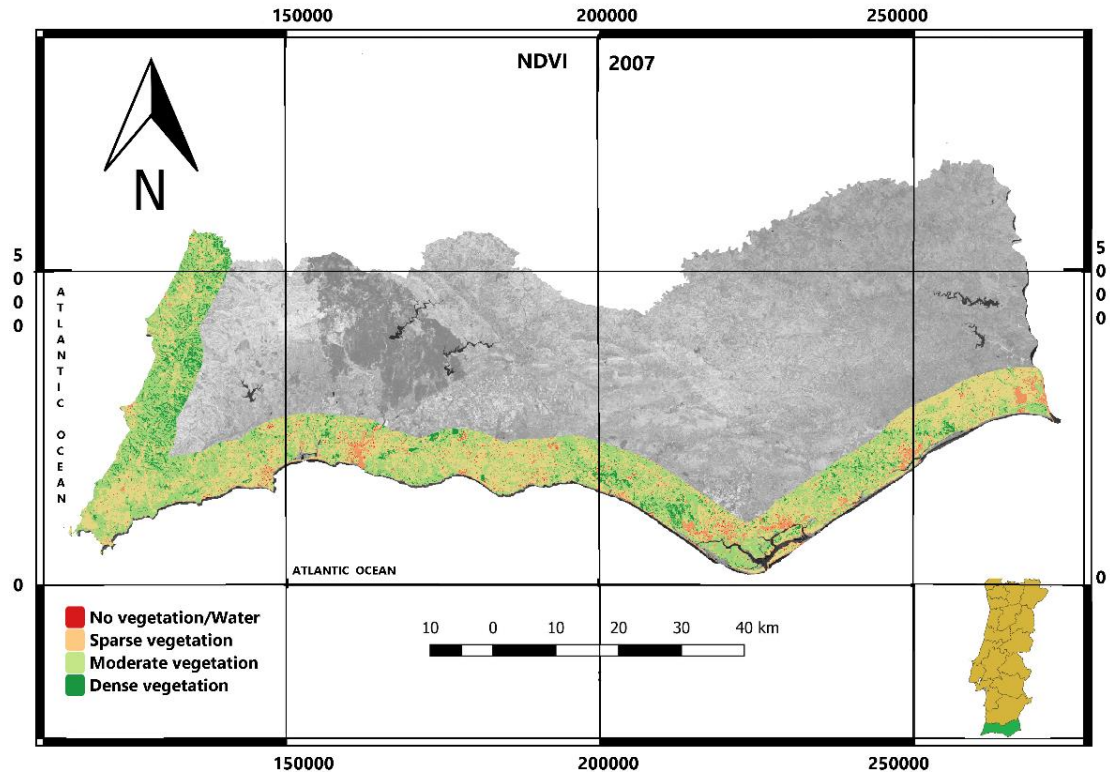

Figure 17: NDVI map from Algarve Coast in 2007 (Source: Elaborated by the Author).

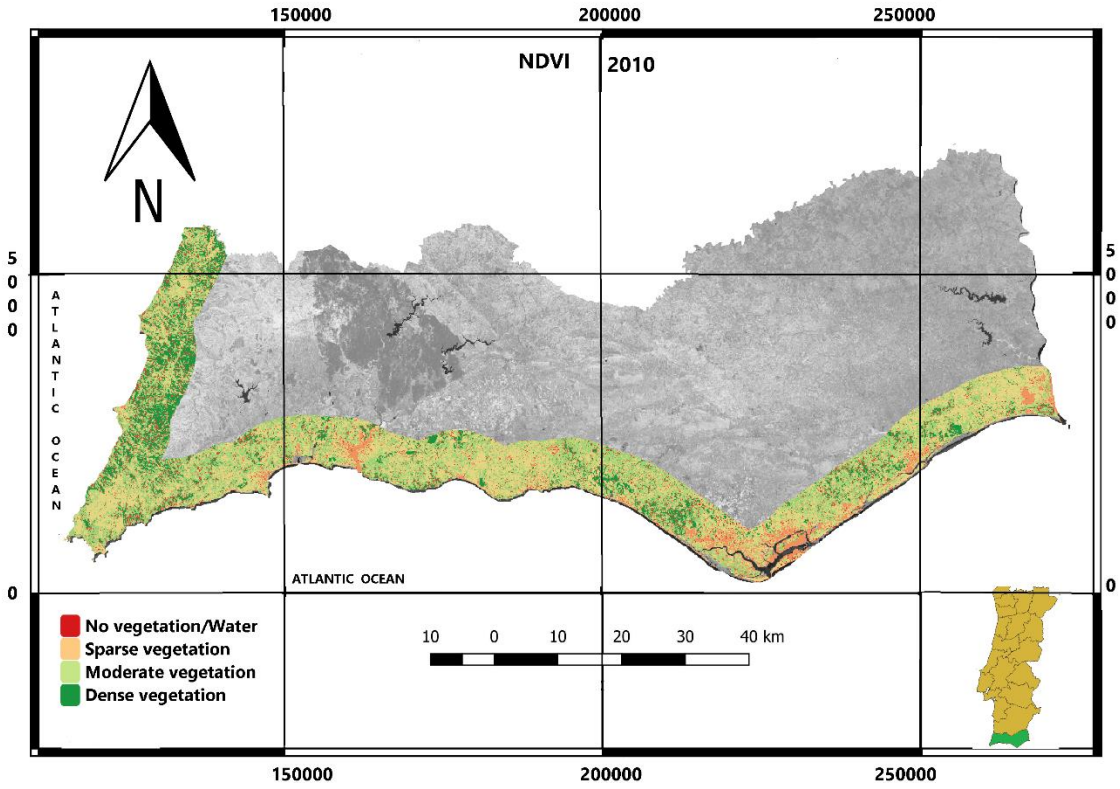

Figure 18: NDVI map from Algarve Coast in 2010. (Source: Elaborated by the Author).

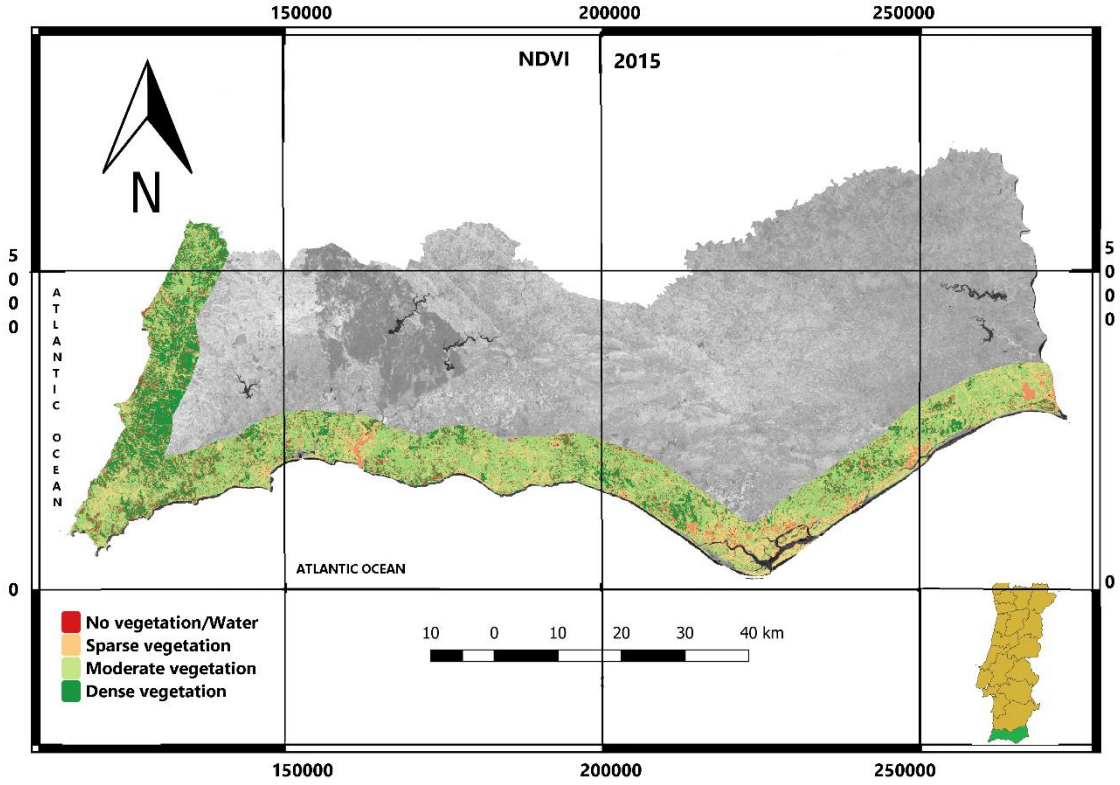

Figure 19: NDVI map from Algarve Coast in 2015. (Source: Elaborated by the Author).

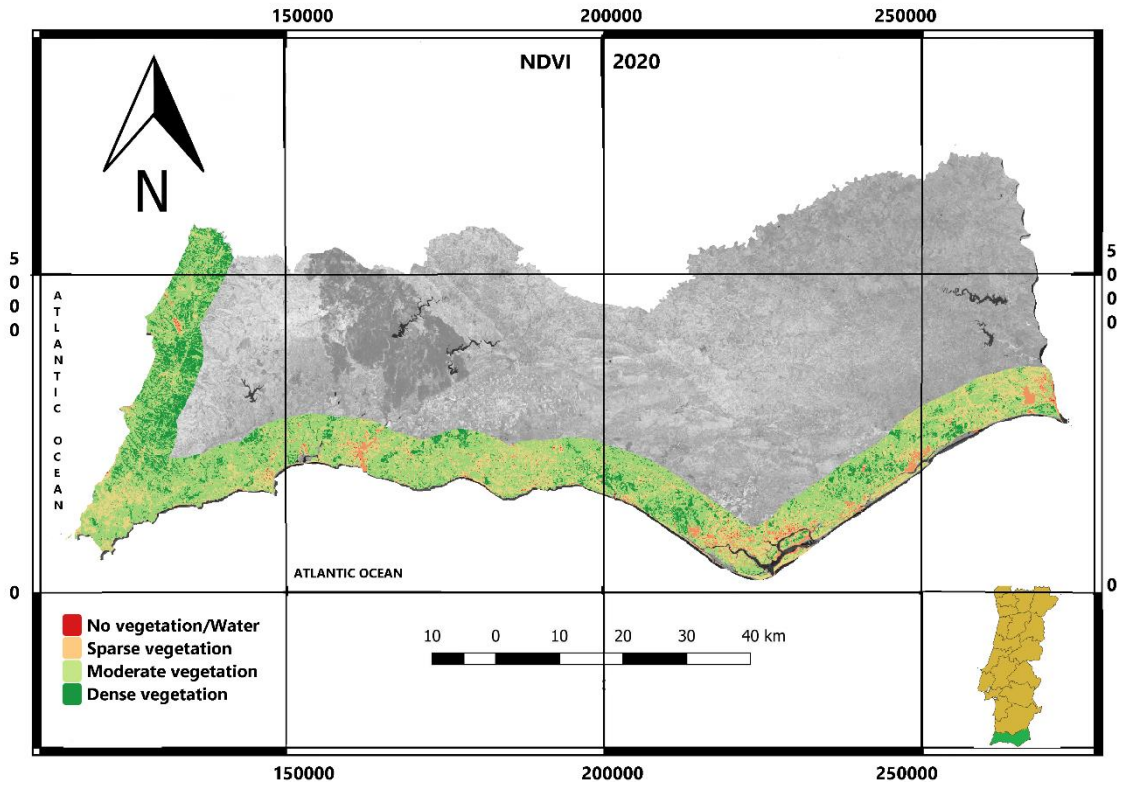

Figure 20: NDVI map from Algarve Coast in 2020. (Source: Elaborated by the Author).

Analysing the maps, we can add that the dense vegetation is most representative in the Vicentina Coast. There are also, other small clusters, namely, Ludo (Faro) and Mata of Conceição (Tavira). However, this class is represented, along south coast, in the golf courses, *e.g.*, Gramacho, Amoreira, Salgados, Vale de Lobo, Quinta do Lago and Quinta da Ria. The class moderate is spread for all south coast of the study area. The class representing the absence of vegetation and waters are in urban areas, salt marshes and salines.

5.2 PRI RESULTS

As mentioned earlier, between 1990 and 2010 data was extracted from the Landsat 5 TM sensor and the Landsat 8 OLI sensor, starting in 2015 (Table 11).

Table 11: PRI Index Values

Year	Satellite/Sensor	PRI Values	Mean	Std Dev.
1990	Landsat 5/TM	0.03 - 0.50	0.04	0.02
1997	Landsat 5/TM	0.02 - 0.26	0.14	0.02
2002	Landsat 5/TM	-0.28 - 0.20	0.12	0.17
2007	Landsat 5/TM	0.17 - 0.73	0.45	0.40
2010	Landsat 5/TM	-0.76 - 0.80	0.02	1.10
2015	Landsat 8/OLI	-0.69 - 0.83	0.07	1.07
2020	Landsat 8/OLI	-0.79 - 0.82	0.01	1.13

Table 11 indicates that the years with the more homogeneity of values was between 1990 and 2007, with a range of standard deviation of 0.02 to 0.40. Between 2010 and 2020, there was greater variation between the extreme values recorded, thus presenting a standard deviation greater than one, which indicates more heterogeneity concerning previous years.

This situation may be due to the greater amount of submerged vegetation in the saltmarshes areas because the recorded tide is higher in those days when the images were captured (Table 5).

Like what was done for the NDVI, the results were reclassified to analyse in more detail, the evolution of areas encompassed by each of the classes to liken with other indices.

Due to the absence of a methodology applicable to the reclassification, as exists for the NDVI (Rahman *et al.*, 2000), was used the Natural Breaks division (Jenks) of ArcMap, based on natural groupings inherent in the data (Table 12 and Figure 21).

Table 12: PRI Reclassification

Class	Range	1990	1997	2002	2007	2010	2015	2020
1- Moderate (negative)	<-0.18	20.2%	28.5%	30%	43.6%	31.5%	28.0%	26.3%
2- Elevated	[-0.18, 0.24[	15.6%	14.0%	15.8%	8.6%	19.0%	19.5%	17.4%
3- Moderate (positive)	[0.24, 0.29]	39.0%	51.0%	49%	45.2%	41.2%	35.8%	34.7%
4- Low	>0.29	25.2%	6.5%	5.2%	2.6%	8.3%	16.7%	21.6%

In the PRI index, values vary between -1 and 1, but for this index, values closer to zero indicate a greater photosynthetic activity, and consequently a greater carbon retention capacity. Healthy vegetation presents values between -0.2 and 0.2 (GAMON *et al.,*1992). Thus, it can be said that class [-0.18, 0.24] is the most efficient in the division.

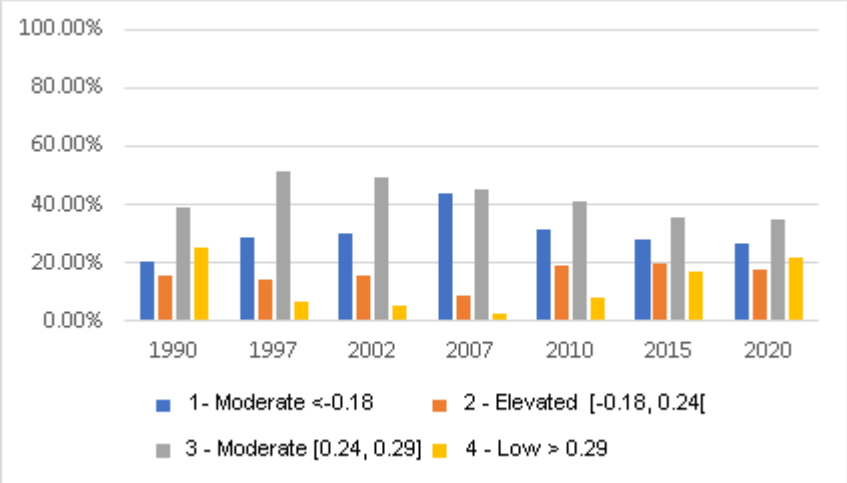

Figure 21: PRI Reclassified values by Natural Breaks division.

Figure 21 shows that the evolution of the classes over the years is like to those of the NDVI, previously presented. Comparing the PRI classes with those of the NDVI, it can be observed that the best levels in photosynthetic efficiency levels is directly linked to the moderate and dense vegetation classes, described in the previous topic.

For class 1, the values recorded throughout the period studied, show areas of occupation between 20% to 30%, with a peak of 43.6% recorded in 2007.

For Class 2, values from the TM Sensor (1990-2010), the percentages of area, was ranged between 8.6% and 19.0%. The OLI Sensor registered similar percentages: 19.5% and 17.4% in 2015 and 2020, respectively.

Class 3 presented, in the three first decades (1990-2010), values close to 40% and 50%. After this period, the records of Sensor OLI (2015 and 2020) showed that the class started to lose representativeness, with occupations around of 35%.

Class 4, according to TM sensor data, in 1990 had in region an ocupation of 25.2%, but in 1997 had a sharp decrease reaching percentages between 2.6% (minimum in 2007) and 8.3% (maximum in 2010). In the years 2015 and 2020, the sensor OLI data showed that class started to have more expression with occupancy values 16.7% and 21.6%, respectively.

The spatial distribution of PRI for the studied period are presented in Figures 22-28.

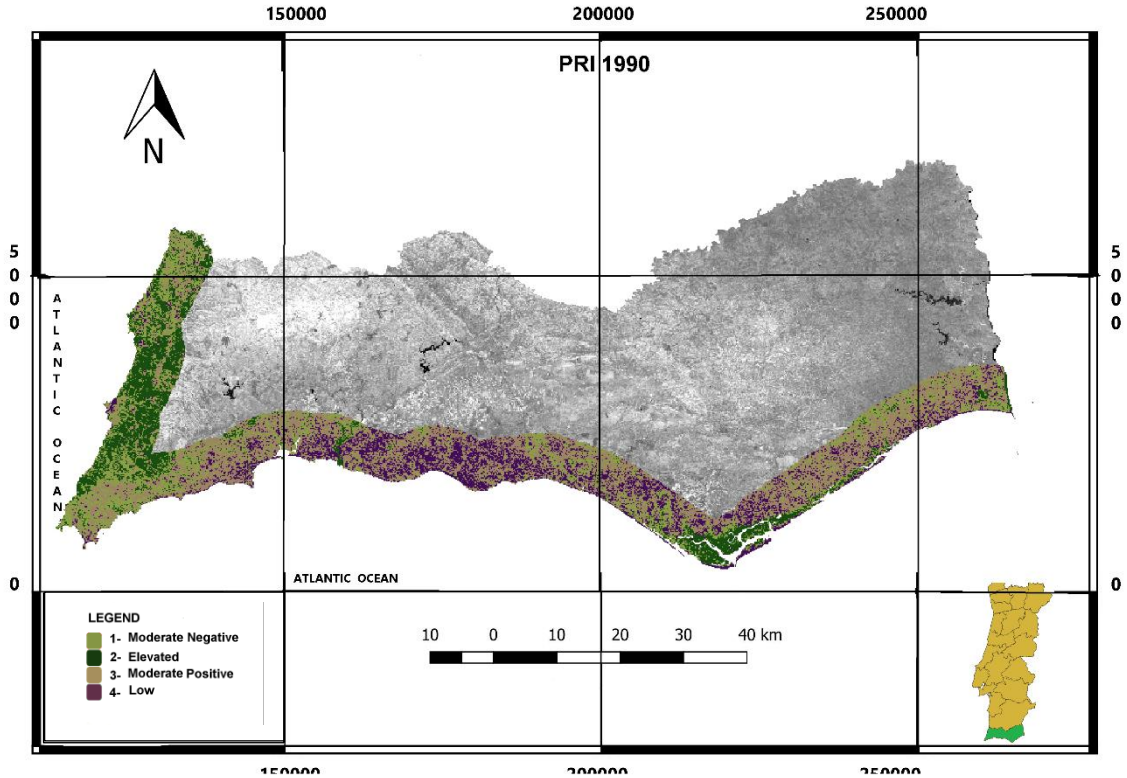

Figure 22: PRI map from Coastal Algarve in 1990 (Source: Elaborated by the Author).

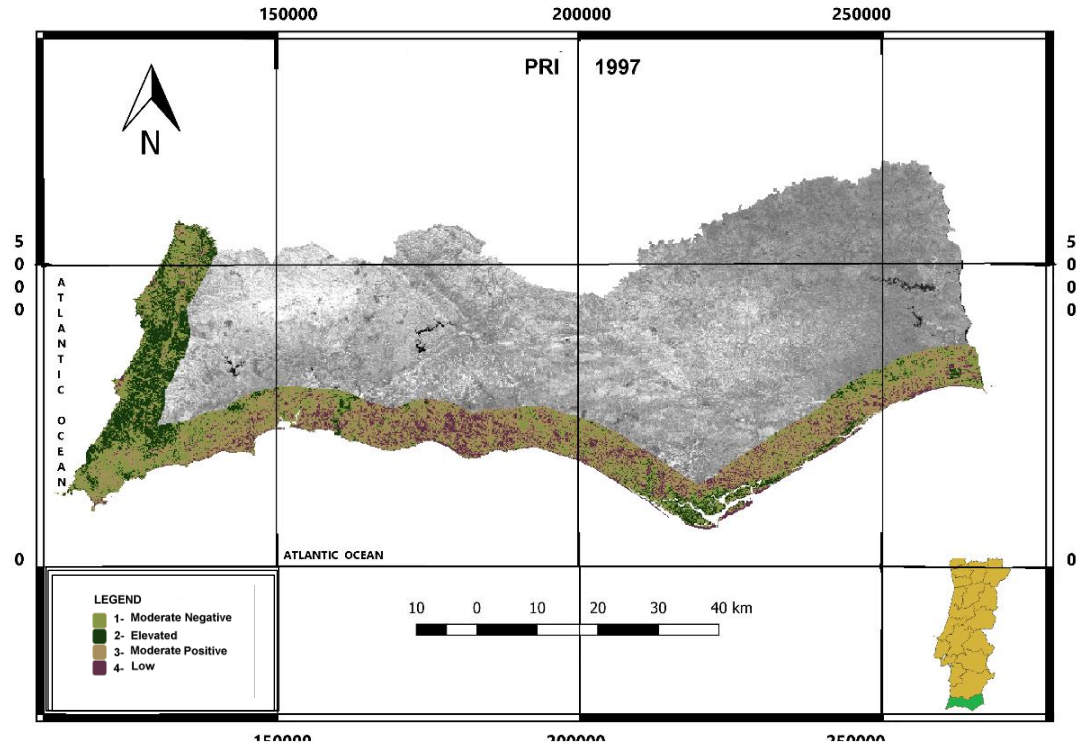

Figure 23: PRI map from Coastal Algarve in 1997 (Source: Elaborated by the Author).

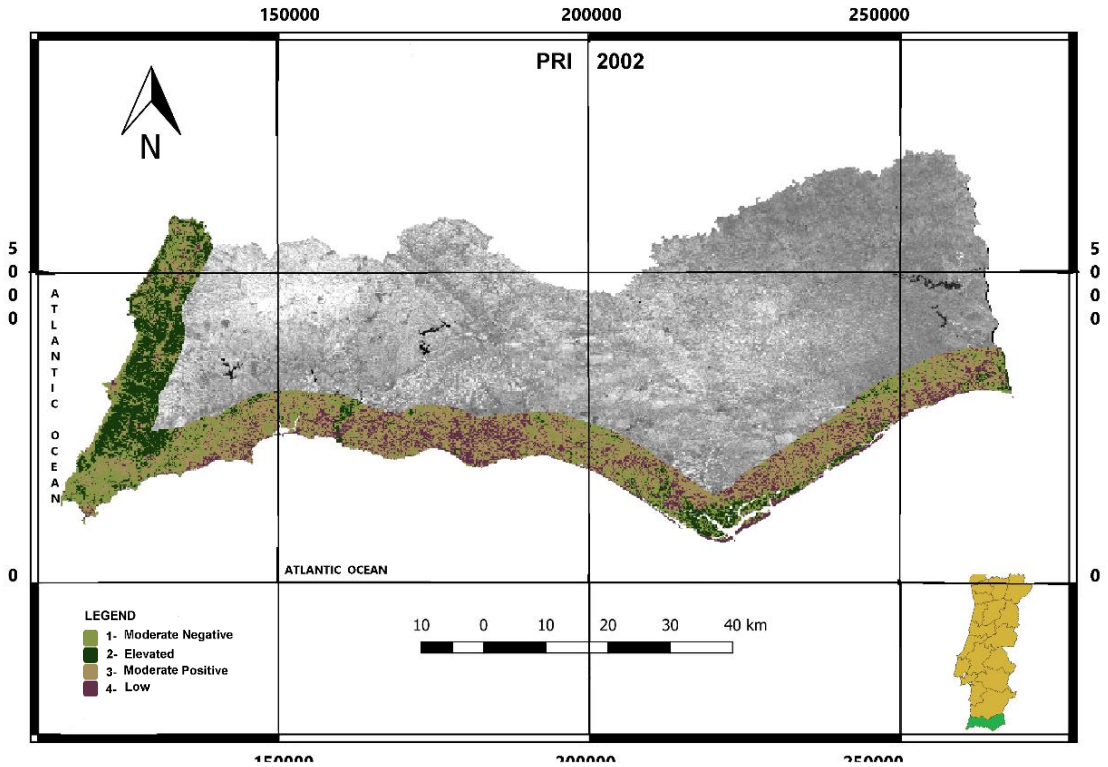

Figure 24: PRI map from Coastal Algarve in 2002. (Source: Elaborated by the Author)

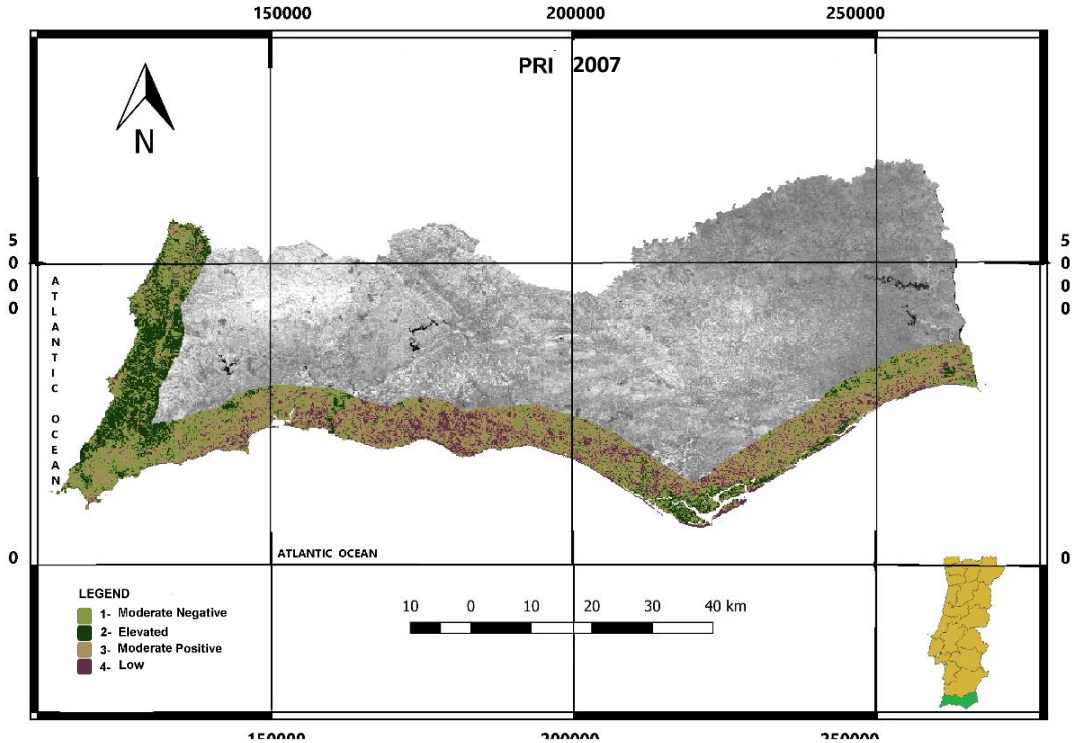

Figure 25: PRI map from Coastal Algarve in 2007 (Source: Elaborated by the Author).

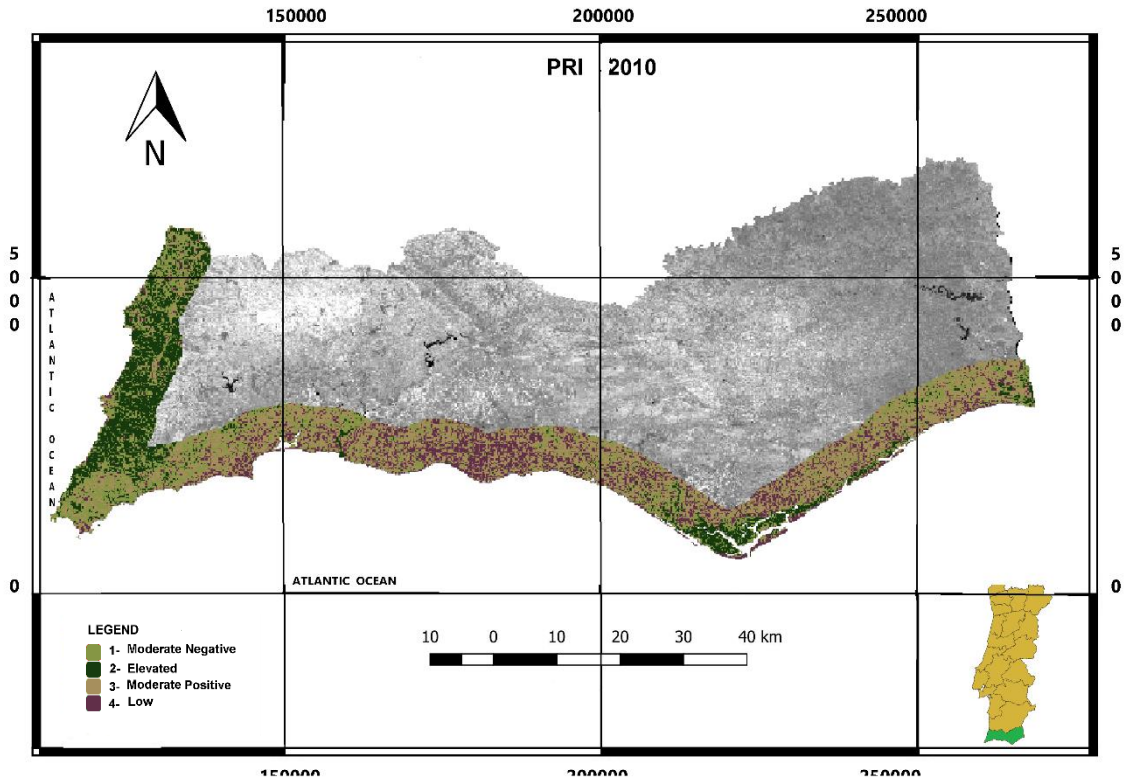

Figure 26: PRI map from Coastal Algarve in 2010 (Source: Elaborated by the Author).

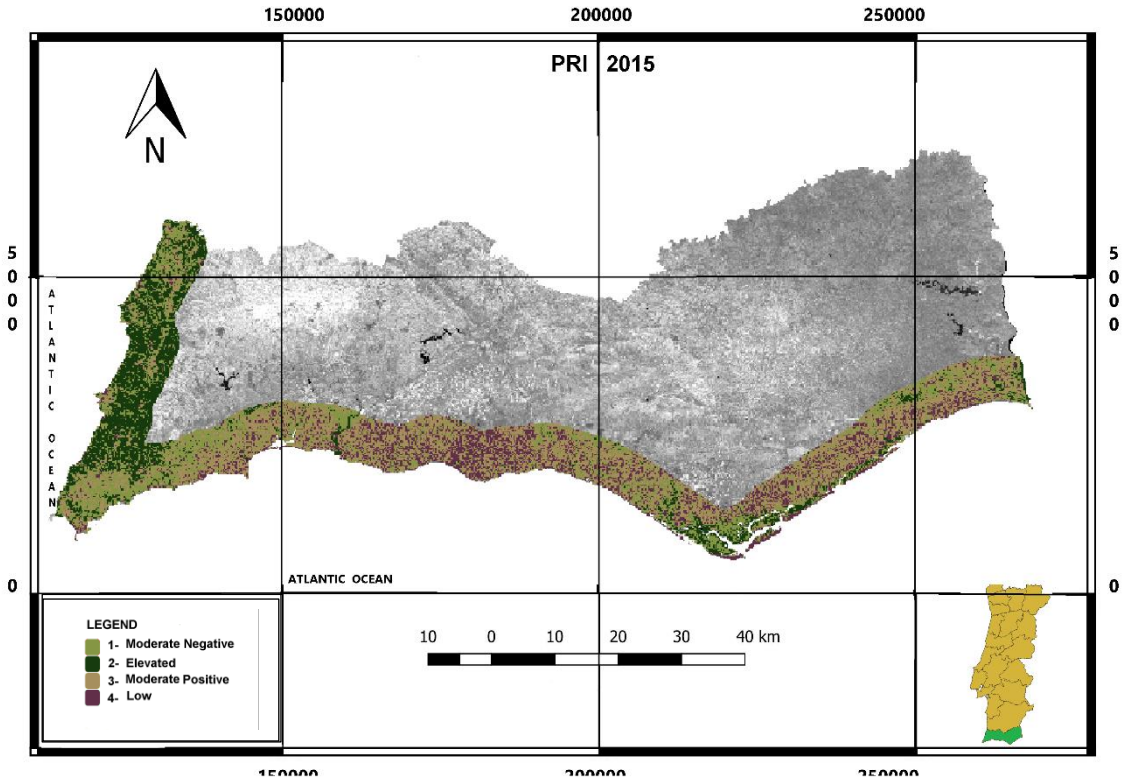

Figure 27: PRI map from Coastal Algarve in 2015 (Source: Elaborated by the Author).

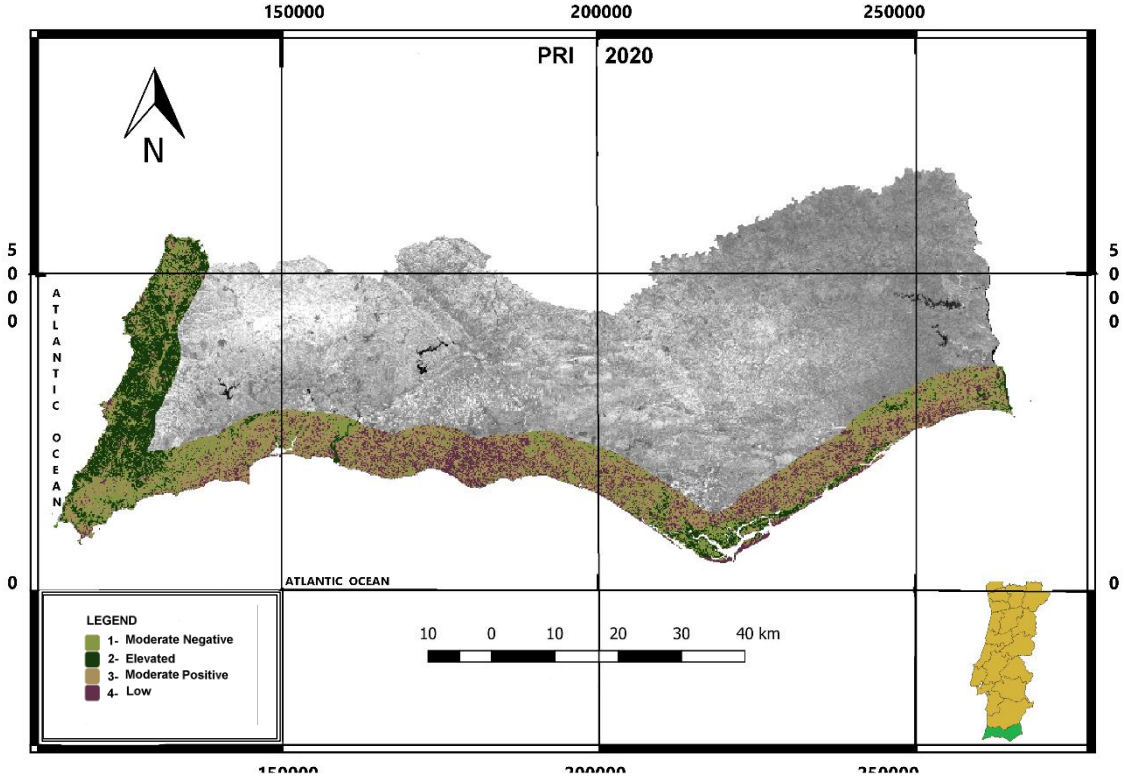

Figure 28: PRI map from Coastal Algarve in 2020 (Source: Elaborated by the Author).

The maps above show a variation between darker and lighter shades of green over the years. This directly expresses the photosynthetic efficiency as a function of on-site radiation use at plants' leaf and canopy levels. According to Coltri *et al.,* 2009; Rahman *et al.,* 2000, the PRI index varies according to the photosynthetic capacity of plants, type of vegetation and efficient use of radiation. When the PRI index values are closer to zero (dark shades of green), the greater the capacity to use light by photosynthesis and, consequently, the greater the efficiency of the plant in carrying it out.

In Costa Vicentina, belonging to the Natura 2000 protected area and in salt marshes of the south coast, it is observed that the variations were not high, remaining, in general, constant. However, it is worth mentioning that there were some changes throughout the period studied in the Ria Formosa area. At the end of the period, there was a decrease in photosynthetic efficiency and consequently the rates of CO_2 retention.

5.3 CO_2FLUX AND GPP RESULTS

Following the methodology of Rahman *et al.* (2000), the CO_2flux Index, previously described, was calculated. Table 13 contains the values obtained for this index.

Table 13 – CO_2flux index results

	1990	1997	2002	2007	2010	2015	2020
Min. value	-0.22	-0.27	-0.20	-0.39	-0.41	-0.22	-0.46
Max. value	0.37	0.34	0.37	0.44	0.42	0.40	0.42
Mean	0.29	0.03	0.08	0.02	0.01	0.09	-0.02
Std. Dev.	0.10	0.43	0.40	0.58	0.58	0.43	0.62

For the Sensor TM, it was found that the CO_2flux values range in the years 1990, 1997 and 2002 went similar. The minimum values were among -0.27 at -0.20 while the maximum values were between 0.34 and 0.37.

Between 2007 and 2010, the values had a significant absolute increase; the minimum levels were between -0.39 and -0.41 and the maximum values in 0.42 and 0.44. Regarding the OLI sensor, 2015 and 2020 kept the maximum

values between 0.40 and 0.42, respectively. The minimum value decreased to -0.22 in 2015 and -0.46 in 2020.

Regarding the GPP data collected by the MODIS sensor, they were reclassified into 5 classes, according to the Natural Breaks algorithm (Jenks). Class 1 represents the minimum input of carbon, while class 5 represents greater carbon retention. Table 14 shows the percentage of occupancy since 2002 (date from which is available information from the GPP MODIS).

Table 14: GPP Class Area Percentage

Class	Range (KgC/m^2×0.0001)	2002	2007	2010	2015	2020
1	[0,166[	4.5%	6.2%	5.6%	3.3%	2.6%
2	]166,276]	26.1%	26.8%	24.4%	22.8%	20.8%
3	]276,400]	38.7%	35.4%	33.2%	33.9%	34.4%
4	]400,756]	19.4%	24.6%	24.0%	28.0%	28.9%
5	>756	11.4%	8.0%	11.8%	12.0%	13.3%

The results above highlight the great similarity and proximity of the values of each class throughout the studied period.

The class 1 is essentially located in waterbodies, and yours ocupation remained stable for the entire studied period, varying between approximately 2.6% and 6.2%.

The class 2, remained between 20.8% (minimum in 2010) to 26.8% (maximum in 2002), with a downward trend from 2007 onwards and was mainly distributed in urban centers.

The class 3, representing average concentrations, was the class with the highest representation, varying between approximately between 38.7% (maximum in 2002) and 33.2% (minimum in 2010). Since 2010 has had a small growth trend .

The class 4, presents lowest area value in 2002 (19.4%) and the highest value in 2020 (28.9%). It has representation in all the territory.

The class 5, appears mainly on the west coast and in ramsar areas, presenting with lowest percentage in 2007 (8%), and its highest in 2020 (13.3%). It has been growing since 2007. The Figure 31, Figure 33, Figure 35, Figure 37 and Fig 39 show the distribution of classes in the study area from 2002 to 2020.

Linear regressions were calculated between the MODIS GPP values, used as a response variable, and the values of the CO_2flux average, used as an explanatory variable for each of the scenarios (Table 15 and Figure 29).

Table 15 – Adjusted values by linear Regressions

Year	R^2	Linear equation
2002	0.56	$y = 2.0228x - 14.013$
2007	0.61	$y = 1.8718x - 20.328$
2010	0.64	$y = 1.4793x + 40.543$
2015	0.66	$y = 2.3186x - 77.991$
2020	0.47	$y = 1.5543x - 5.0384$

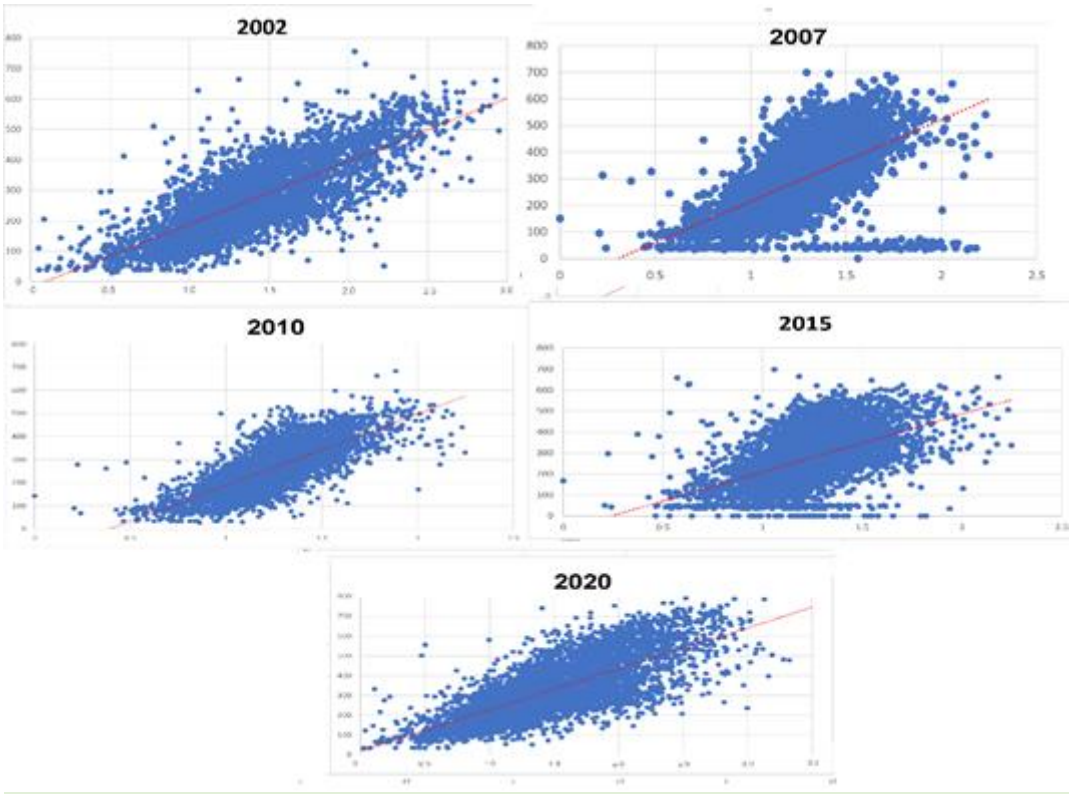

Figure 29: Scatter Plots from the adjustments.

The best adjustments were in 2015 (R^2=0.66) and 2010 (R^2=0.64), and the lowest in 2002 (R^2 =0.56) and 2020 (R^2= 0.47).

The GPP data with a resolution of 30 m obtained from the linear regression were also reclassified applying the Natural Breaks division (Jenks). Table 16 and Figure 30 contains the variation of area percentage of occupation for each class since 2002.

Table 16 - GPP with a resolution of 30 m obtained from the linear regression

Class	(KgC/m²×0.0001)	2002	2007	2010	2015	2020
1	[0, 166]	1.5%	1.2%	2%	1.6%	1.3%
2	]166-276]	23.6%	27%	24.4%	23%	20.5%
3	]276-400]	39.2%	38%	38%	38.5%	38.3%
4	]400-756]	24.3%	24.5%	24%	25%	27.5%
5	>756	11.4%	8.8%	11.8%	12%	12.5%

Figure 30: Graph expressing the GPP (with a resolution of 30 m obtained from the linear regression) percentage variation over the time series.

The results of Table 16 presents throughout the studied period more similarity than the GPP MODIS data.

Class 1, represents the water bodies, and remains stable, close to 2%, corroborating the results of the other indices calculated so far. Class 2, can be compared with the sparse vegetation areas of the NDVI. Remains stable, with low variation over the period. It is worth mentioning 2007, with the highest area (27%) and 2020 with the lowest area recorded (20.5%). Class 3, equivalent to moderate vegetation, presented percentage areas with values between 38.0% and 39.2% for the years observed. Classes 4 and 5 , which represent the areas with the highest carbon retention, remained at around 24.0% (2010) to 27.5% (2020) and 8.8% (2007) to 12.5% (2020), respectively. These percentages increased in the studied period, following the trend of the other indexes.

The spatial representation of MODIS GPP and the Adjusted Model for CO_2flux are represented in Figures 31-40.

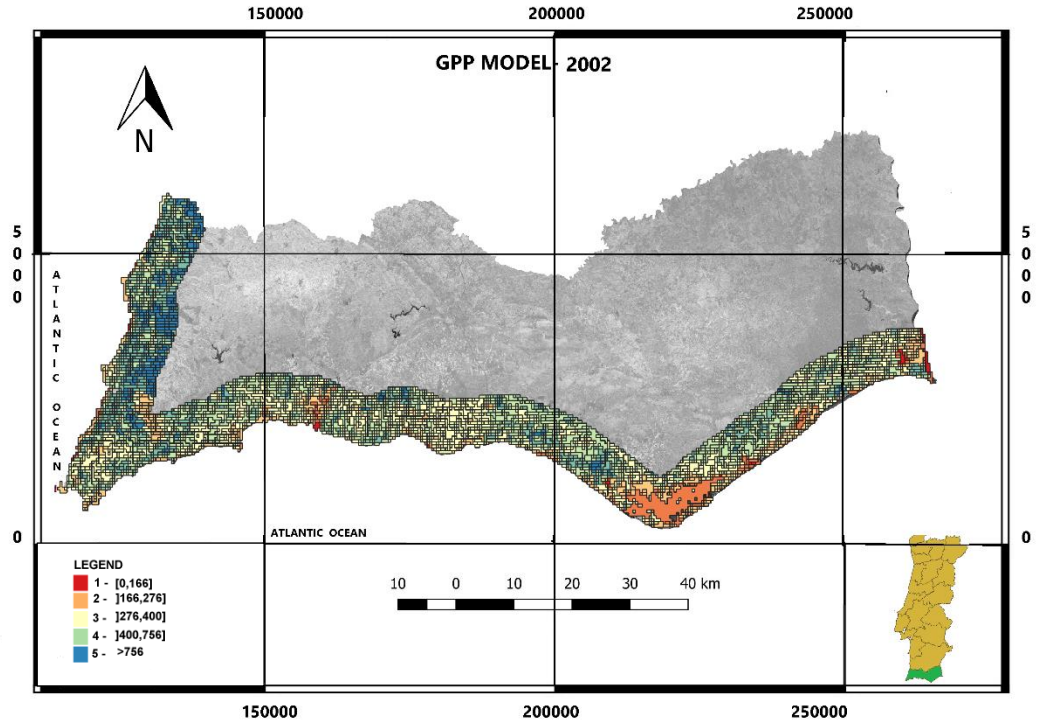

Figure 31: GPP model for 2002 in *KgC /m²×0.0001* units (Source: Elaborated by the Author).

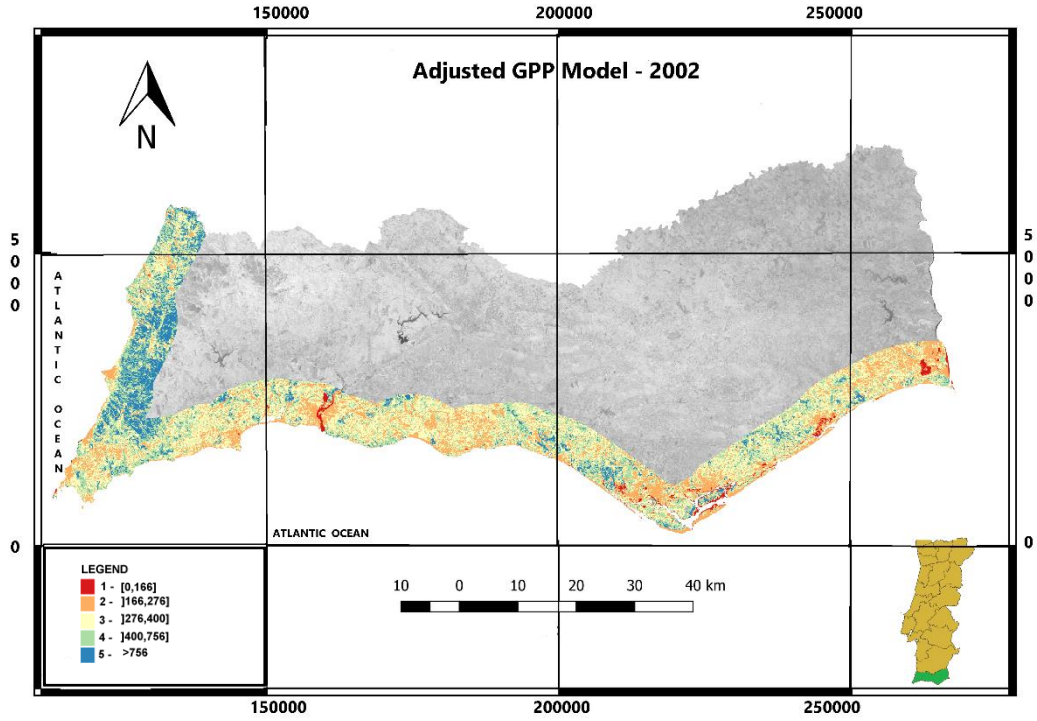

Figure 32: GPP vs. CO_2flux adjusted model for 2002 (Source: Elaborated by the Author).

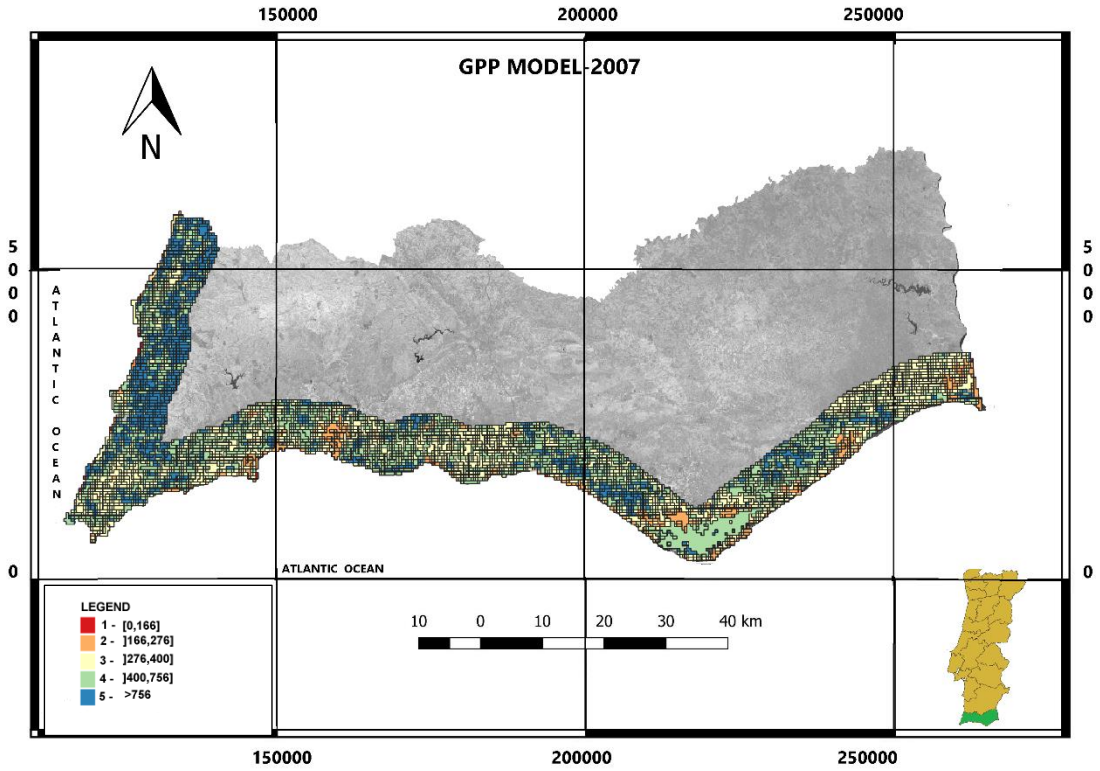

Figure 33: GPP model for 2007 in KgC /m^2×0.0001 units (Source: Elaborated by the Author).

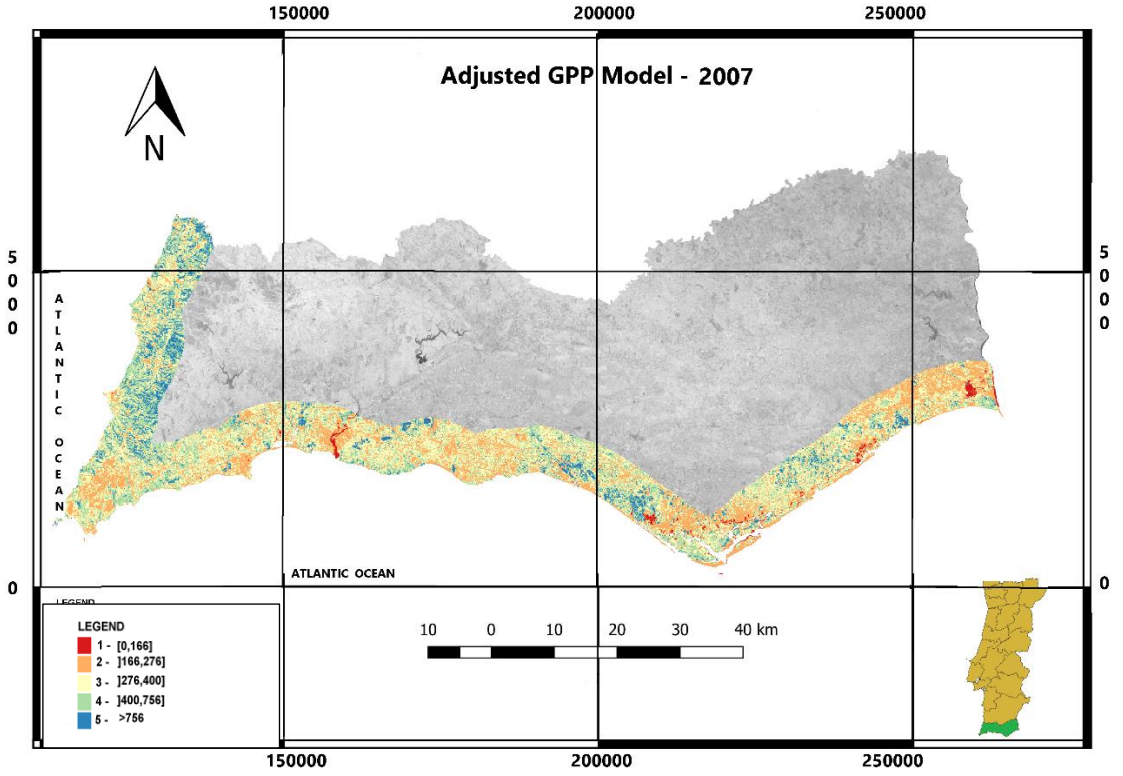

Figure 34: GPP vs. CO_2flux adjusted model for 2007 (Source: Elaborated by the Author).

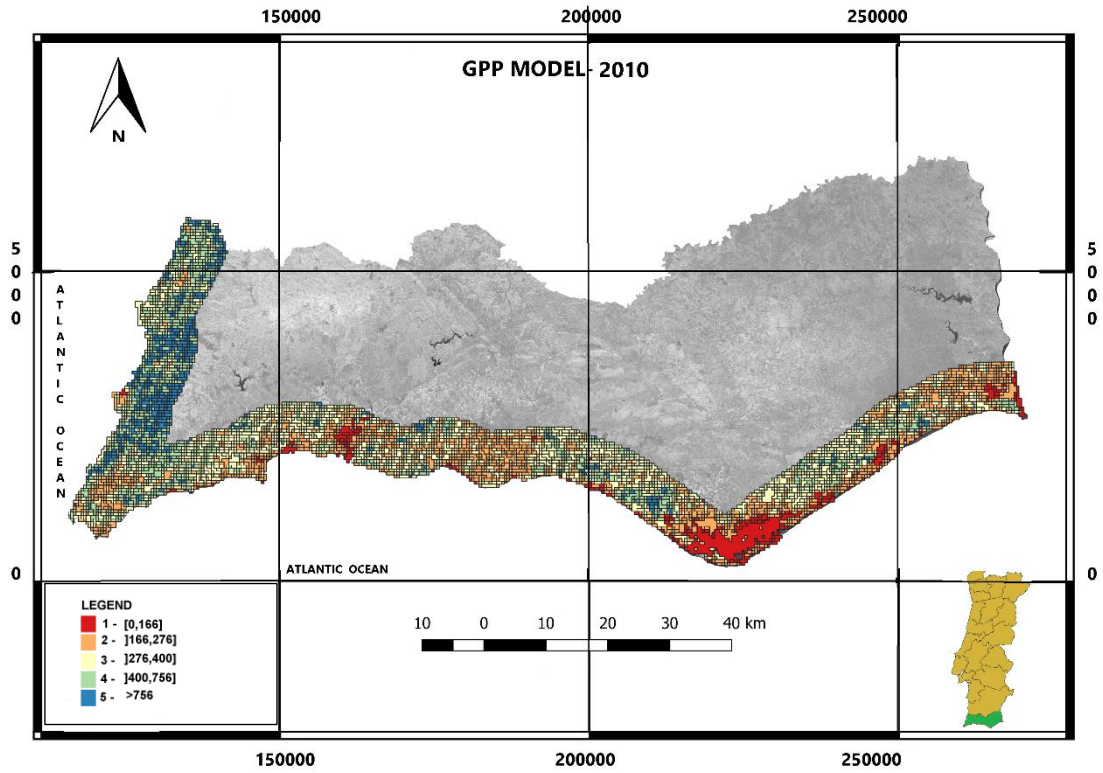

Figure 35: GPP model for 2010 *in KgC /m²×0.0001* units (Source: Elaborated by the Author).

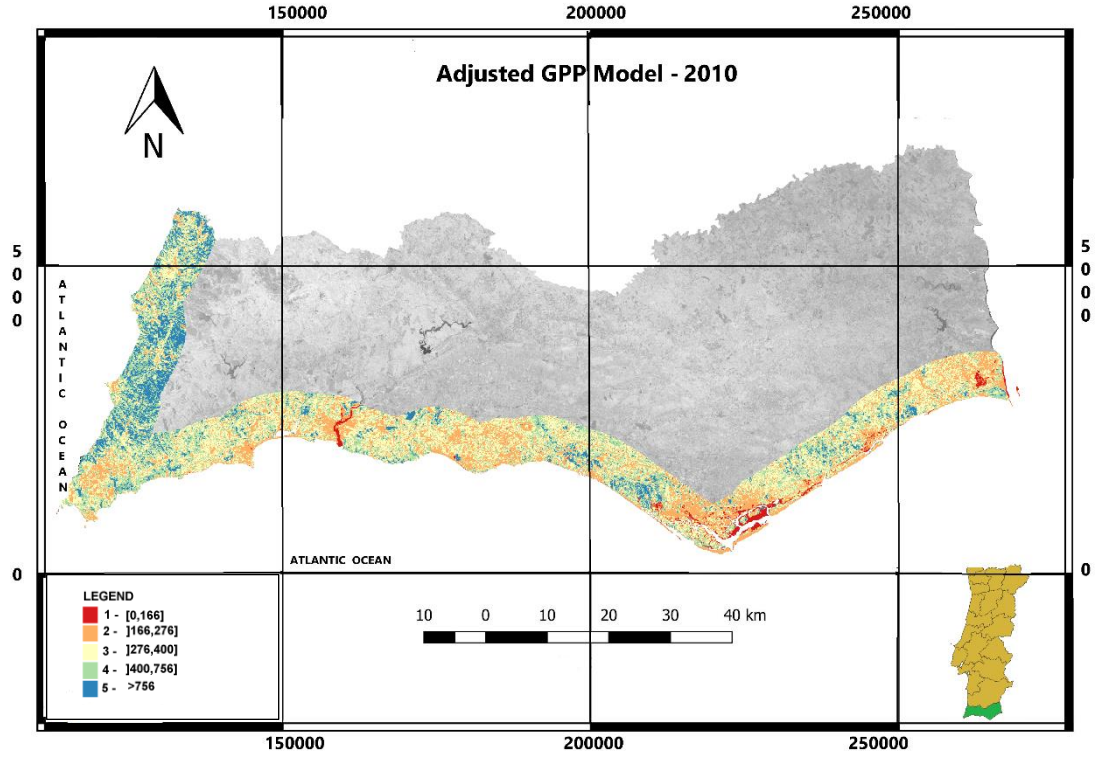

Figure 36: GPP vs. CO_2flux adjusted model for 2010 (Source: Elaborated by the Author).

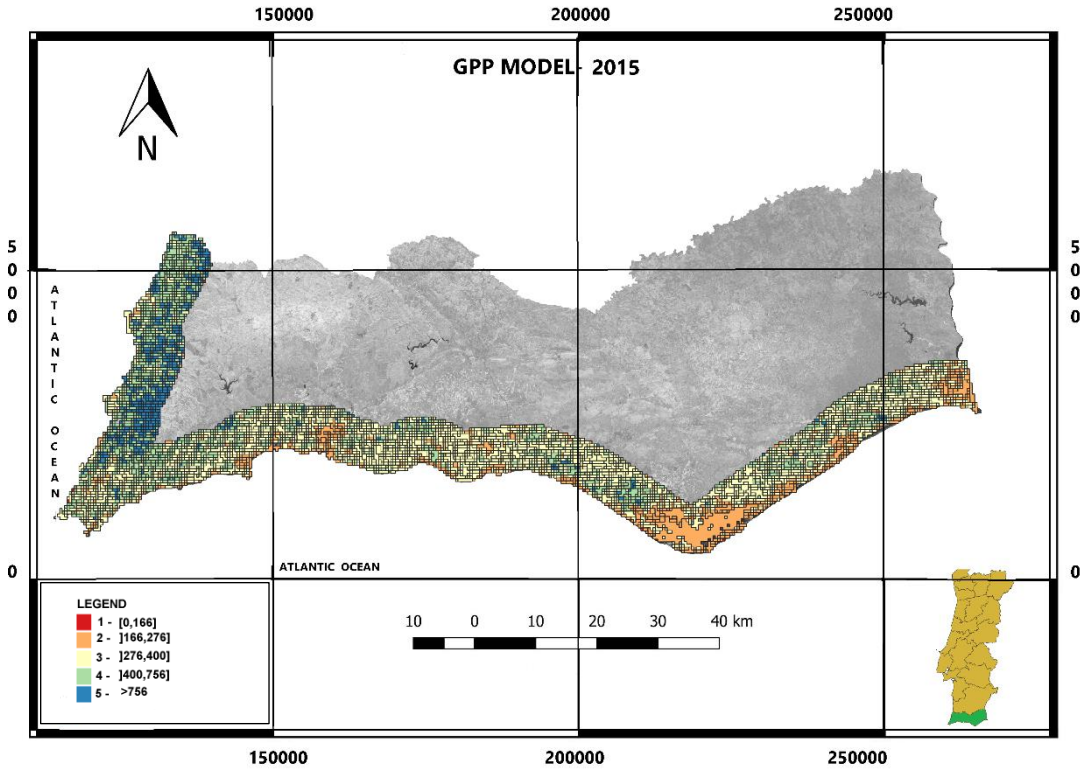

Figure 37: GPP model for 2015 *in KgC /m²×0.0001* units (Source: Elaborated by the Author).

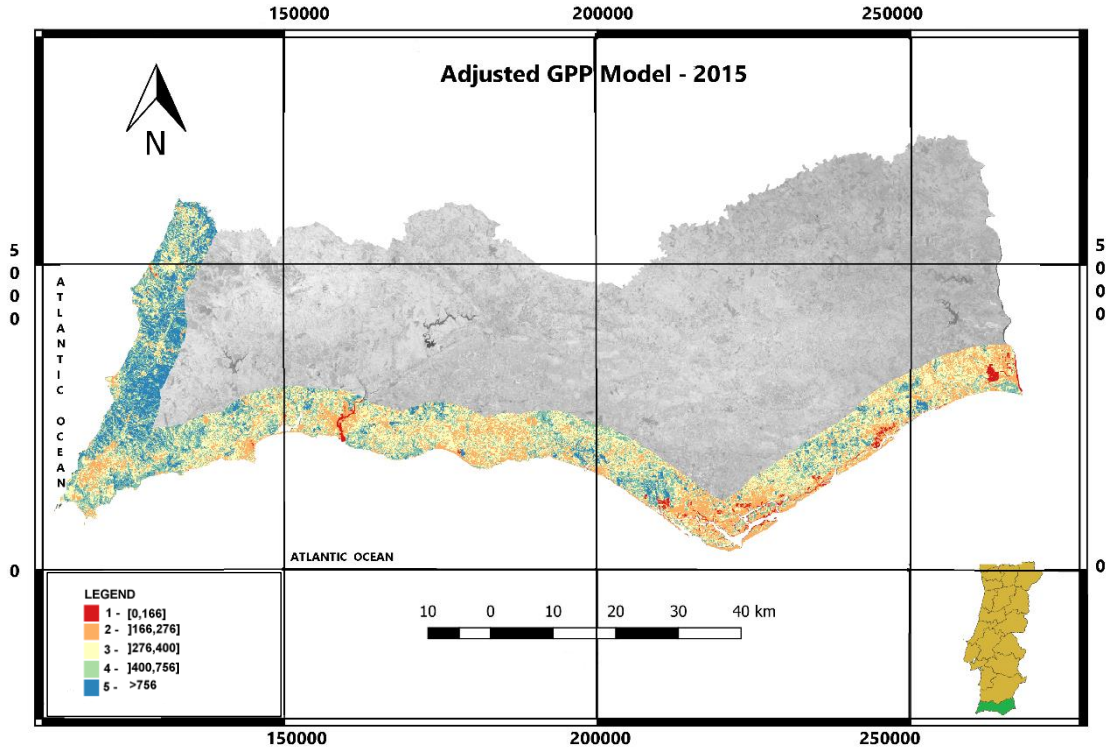

Figure 38: GPP vs. CO_2flux adjusted model for 2015 (Source: Elaborated by the Author).

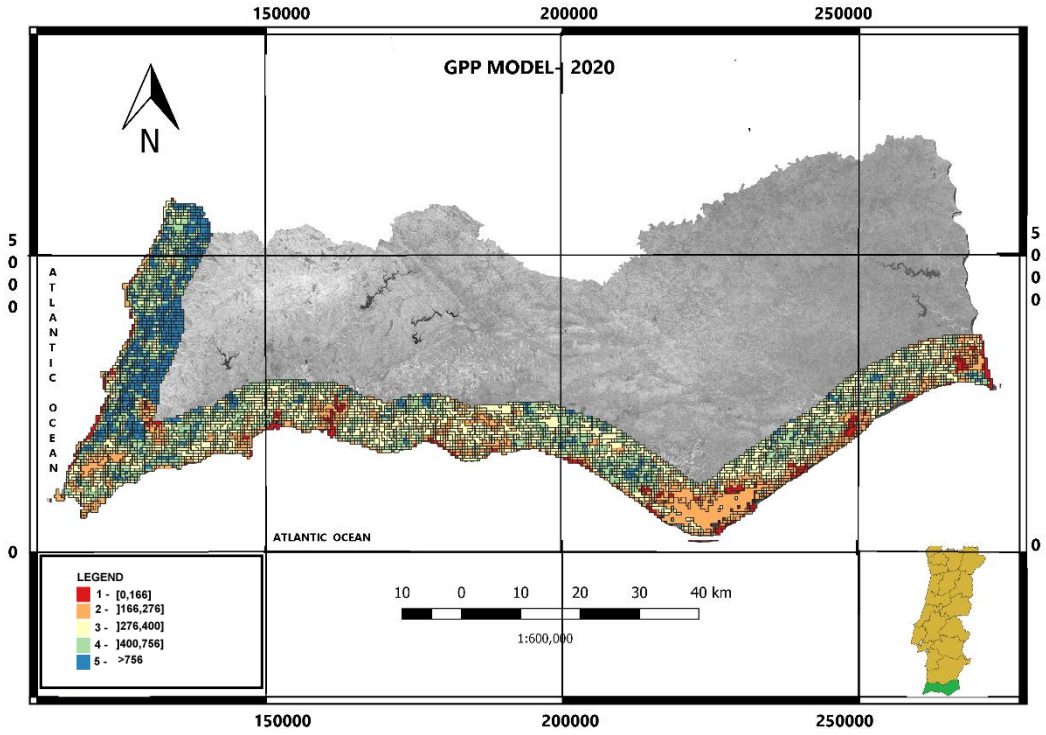

Figure 39: GPP model for 2020 *in KgC /m²×0.0001* units (Source: Elaborated by the Author).

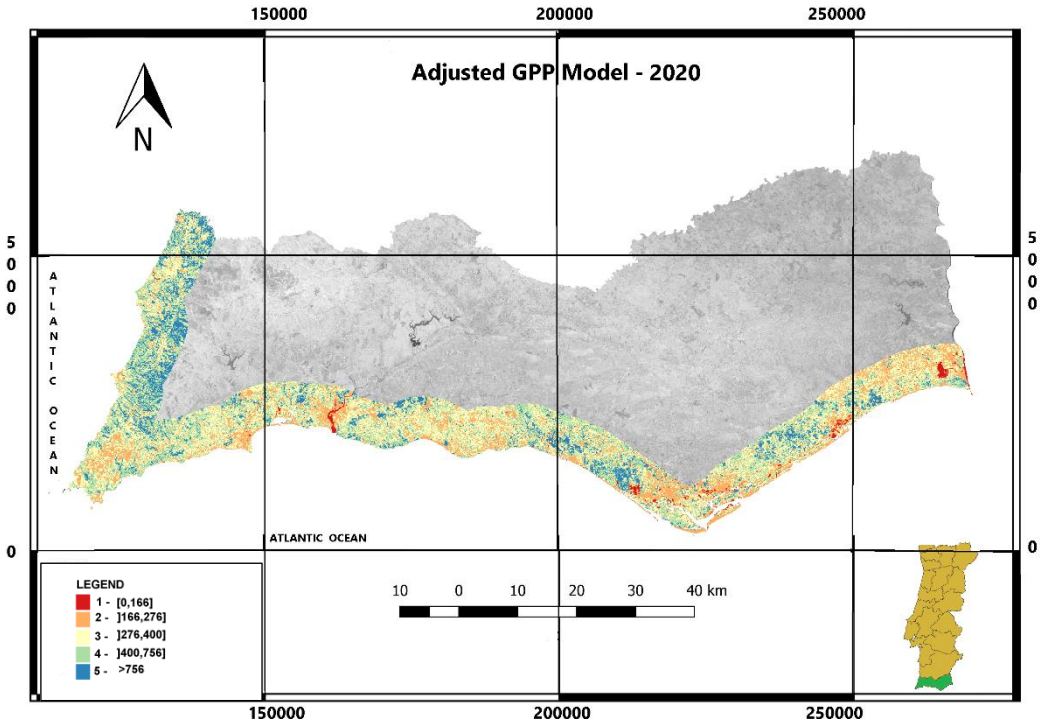

Figure 40: GPP vs. CO_2flux adjusted model for 2020 (Source: Elaborated by the Author).

When compared the maps adjusted by linear regression with GPP map, derived from the MODIS sensor, we can observe a similarity in the distribution of the patches for the same areas. The NDVI, PRI, CO_2flux and the GPP models, are analogous and directly proportional. The high NDVI values, indicate greater density of the vegetation, and in these areas the PRI is also high, that show there is a high photosynthetic activity, and consequently a great retention of CO_2, represented by high values of CO_2flux and GPP (Vicentina Coast and Ramsar areas). The same happens with the low values of the indices, which indicate low vegetation density, low photosynthetic activity, which perform into low levels of CO_2flux and GPP (urban areas and water bodies zones).

5.4 CORINE LAND COVER RESULTS

Below is a summary of the results obtained, expressed in the following Table 17 and Figure 41.

Table 17: CLC Classes Percentages

Classes	1990	2000	2006	2012	2018
Urban	6.4%	11.6%	12.7%	12.8%	15.9%
Farming	60.1%	53.7%	50%	49.3%	46.6%
Vegetation	25.1%	27%	29%	29.4%	29.1%
Wetlands Zones	7.2%	7%	7.3%	7.3%	7.3%
Water Bodies	1.2%	0.7%	1%	1.2%	1.1%

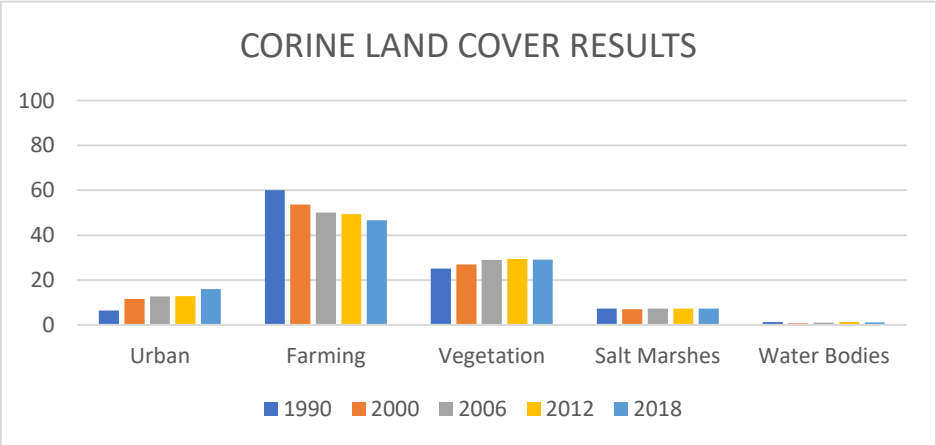

Figure 41: Corine Land Cover class percentage distribution (Source: Elaborated by the Author).

According to the results displayed, it is possible to infer that the urban expansion in the study area had a significant increase since the 2000s, jumping from 6.4% of the occupation of the territory in 1990 to 11.6%. Since then, the growth of this category has continued at a slow pace, increasing only 4.3% in 18 years.

The areas destined for agriculture correspond to the group of greater representation. However, it is possible to observe the decline in the use of these areas. In 1990, they occupied 60.1% of the entire territory, and, since the 2000s, there has been a significant reduction, going to 46.6% in 2018.

The vegetation cover, in general, has increased. Gradually rising from 25.1% in 1990 to 29.1% in 2018. It can also be concluded that the natural areas where the protected areas of the Ramsar Sites and the Natura 2000 network are located have not undergone major changes over the period.

The area occupied by freshwater bodies in the study area did not undergo significant changes, remaining around 1%.

6 DISCUSSION

6.1 VEGETATION INDEXES VALUES AND ITS ENVIRONMENTAL MEANING

This work focused on coastal areas, where most of the population is concentrated, which is why these areas are of extreme economic and social importance and, consequently, are the areas that suffer the most from anthropic pressure. In these areas, too, are located the main wetlands and forests that have an essential ecological role in carbon sequestration.

A quantitative description of the biomass distribution is essential for making the carbon sequester stock, modelling the global biogeochemical cycles, and understanding the historical effects and impacts of human activities (Bar-On & Milo, 2018). The same author states even though the primary production of terrestrial and marine environments is very close, the production of biomass from terrestrial environments is about two orders of magnitude greater in marine biomass.

This work used images from the Landsat program, namely Landsat 5 (TM sensor) and Landsat 8 (OLI sensor), to avoid unconformity in reflectance values. In addition, the images had a calibration Top-of-Atmosphere (TOA) reflectance based on NASA/USGS protocol.

This work showed a gain in biomass and vegetative vigour in all study areas, particularly for the Ramsar sites and Natura 2000 site, which indicate that these locations present ecological homeostasis and that public preservation policies are being followed. Furthermore, the decrease of areas without vegetation and sparse vegetation was compensated by increasing moderate and dense vegetation areas.

Crossing the NDVI and PRI results was found a correlation between these indexes. The highest rates of photosynthetic efficiency occur in the same areas where there is a higher vegetation density, thus indicating a healthy state of the plants. These areas are on the west coast and leisure (golf courses). The lowest values for the PRI are in urban regions, where vegetation cover is low or non-existent. The CO_2flux and GPP show a cyclical variation in biomass and

vegetation vigour production along the Algarve coast. By analysing the graphs and the respective maps, it is possible to observe that the region is an extensive carbon reservoir. However, there was a decrease in the efficiency of the carbon sequestration process in urban areas, where the concentration of vegetation is low.

The criteria for the low tide were chosen for each Landsat image. However, analysing the CO_2flux maps for in time series study, in mainly 2010, 2015 and 2020, found that the wetlands remained at low levels. Therefore, it may be inferred that the tide level is not too low when the data was collected by the satellites.

6.2 CORINE LAND COVER

The results obtained from the analysis of the Corine Land cover are according to the results obtained by the vegetation indexes previously discussed. NDVI, PRI, CO_2flux and GPP had a rise related to the increase of the vegetation class in the studied period.

The social and economic evolution during the last three decades must be considered in the analysis of results, namely, the rate of the population that abandoned agriculture and migrated to other sectors of economic activity, issues related to migratory flows that influenced the expansion of urban centres and ageing population in rural areas. As a result, the areas occupied by vegetation have grown by approximately 4% in three decades; the agriculture areas destined had a decrease of approximately 13.5%; and urban areas expanded by about 9.5%. These results show that agricultural areas were replaced with urbanised areas or abandoned, which gave way to ecological succession, which gradually made the natural vegetation occupy the space of the areas previously used for agriculture.

The new urban areas that include golf courses and resorts contribute for growth solid urban waste, sewage, energy consumption, gas emissions, and, mainly, water use for irrigation of green landscapes. These places showed high NDVI values during the dry period, proving that they were irrigated to maintain good visual quality.

During time series studied, in the environmental protection areas, like the Ramsar and Natura 2000 Sites, present in the Algarve Littoral, namely, Sapais de Castro Marim, Ria Formosa, Ria de Alvor and Vicentina Coast, showed a similitude in occupation of the areas along of the years. The NDVI and GPP values demonstrate this fact, which does not show significant changes in this period. Therefore, it is concluded that the European Union programs are being followed.

6.3 CONTRIBUTION FOR FURTHER WORKS

In this work, a multidisciplinary approach was used, which involved Remote Sensing techniques, Geographic Information systems, geospatial analysis, Biology and Ecology principles for the entire Littoral zone of the Algarve. Faracini (2017) used a similar approach to calculate the vegetation indexes and GPP in a Ria Formosa area and presented similar results.

It is worth mentioning that it is necessary to deepen the results presented here, such as:

- Comparative studies between different periods on the calculation of the NDVI Index specifically focused on golf courses and their general contribution in the values presented here, compared to water consumption, specifically designed for this purpose.
- Application of Change Detection models with predictions for land use and coverage, expansion of urban areas, and assess vegetation's shrinkage, expansion, and vigour.
- Crossing with the data obtained here, with the pluviometry time series and with other climatic factors, since it is a coastal area, with a constant and dependent connection with the factors of the marine systems, so that it can be compared with the effects of desertification, which, as already mentioned, is one of the large-scale problems present in the biomes of the Iberian Peninsula.

The results presented here, and the proposals mentioned above are of great importance so that decision-makers and politicians can base themselves on planning, mitigating and restorative actions so that the Algarve Coastal region can be preserved for future generations.

REFERENCES

Alvarenga, B. S., D'ARCO, E. N. Z. O., Adami, M., & Formaggio, A. R. (2003). O ensino de conceitos e práticas de espectroradiometria laboratorial: estudo de caso com solos do Estado de São Paulo. *Simpósio Brasileiro de Sensoriamento Remoto*, *11*, 739-747.

Alves, F. L., Sousa, L. P., Almodovar, M., & Phillips, M. R. (2013). *Integrated Coastal Zone Management (ICZM): a review of progress in Portuguese implementation. Regional Environmental Change, 13(5), 1031–1042.* doi:10.1007/s10113-012-0398-y.

Anderson, L. O., Latorre, M. L., Shimabukuro, Y. E., Arai, E., & Carvalho Júnior, O. D. (2003). Sensor MODIS: uma abordagem geral. São José dos Campos: INPE, 58.

Andrade, D.D. de.; Ferreira, M.C.; Bolfe, E.L.Estimativa e mapeamento de Carbono em fragmentos florestais da APA Fernão Dias (MG) com uso de dados orbitais do Sensor TM-Landsat. Anais. XV Simpósio Brasileiro de Geografia Física aplicada: Uso e ocupação da terra e as mudanças das paisagens. Vitória (ES), 8 a 12 de julho de 2013. UFES.

Andrade, C., Fonseca, A., & Santos, J. A. (2021). Are land use options in viticulture and oliviculture in agreement with bioclimatic shifts in Portugal. *Land*, *10*(8), 869.

Aníbal, J., Gomes, A., Mendes, I., & Moura, D. (2019). Ria Formosa: challenges of a coastal lagoon in a changing environment.

Araya, Y. (2009). *Urban Land Use Change Analysis and Modeling: A Case Study of Setúbal and Sesimbra, Portugal*. 72.

Asokan, A., & Anitha, J. (2019). Change detection techniques for Remote Sensing applications: a survey. *Earth Science Informatics*, 143–160. https://doi.org/10.1007/s12145-019-00380-5. accessed in 17/03/2020.

Barnsley, M. J., Moller-Jensen, L., & Barr, S. L. (2000). Inferring urban land use by spatial and structural pattern recognition. Remote Sensing and Urban Analysis, London: Taylor and Francis, 115-144.

Batista, C. M., Suárez, A., & Saltarén, C. M. B. (2017). Novel method to delimitate and demarcate coastal zone boundaries. *Ocean & Coastal Management*, *144*, 105-119.

Bar-On, Y. M., Phillips, R., & Milo, R. (2018). The biomass distribution on Earth. Proceedings of the National Academy of Sciences, 115(25), 6506-6511.

Baptista, G. M. M. Validação da Modelagem de sequestro de carbono para ambientes tropicais de cerrado, por meio de dados Aviris e Hyperion. In: Simpósio Brasileiro de Sensoriamento Remoto (SBSR), 11., 2003, Belo Horizonte. Anais São José dos Campos: INPE, 2003. Artigos, p. 1037-1044. Disponível em: http://marte.dpi.inpe.br/col/ltid.inpe.br/sbsr/2002/09.07.21.45/doc/10_002.pdf. Accessed 14/11/2020.

Baptista, G. M. de M., Bento-Gonçalves, A., & Vieira, A. (2018). Avaliação das condições de verdor, umidade e de senescência da vegetação queimada no incêndio de Braga, Portugal, em outubro de 2017. *Desafios Para Afirmar a Lusofonia Na Geografia Física e Ambiente. II Encontro Luso-Afro-Americano de Geografia Física e Ambiente*, 1079–1085.

Bastos, A., Janssens, I. A., Gouveia, C. M., Trigo, R. M., Ciais, P., Chevallier, F., Peñuelas, J., Rödenbeck, C., Piao, S., Friedlingstein, P., & Running, S. W.

(2016). European land CO2 sink influenced by NAO and East-Atlantic Pattern coupling. *Nature Communications*, *7*. https://doi.org/10.1038/ncomms10315. accessed 23/0/2021.

Batten, G. D. (1998). Plant analysis using near-infrared reflectance spectroscopy: the potential and the limitations. Australian Journal of Experimental Agriculture, 38(7), 697-706.

Barker, J.L.; Harden, M.K.; Anuta, E.A.; Smid, J. e Hough, D. MODIS spectral sensitivity study: requirements and characterization. Washington: Nasa, Oct 1992, 84p.

Barbosa, C. C. F., de Moraes Novo, E. M. L., & Martins, V. S. (Eds.). (2019). *Introdução ao Sensoriamento Remoto de Sistemas Aquáticos: princípios e aplicações* (Vol. 1). Instituto Nacional de Pesquisas Espaciais.

Bureau, R. (2001). Wetland Values and Functions.

Bernardes, J. P. (2011). A Cidade de Ossónoba e o SeuTerritório. *Anais do Municipio de Faro*, 11-26.

Borre, J. V., Paelinckx, D., Mücher, C. A., Kooistra, L., Haest, B., De Blust, G., & Schmidt, A. M. (2011). Integrating Remote Sensing in Natura 2000 habitat monitoring: Prospects on the way forward. Journal for Nature Conservation, 19(2), 116-125.

Bossard, M., Feranec, J., & Otahel, J. (2000). CORINE land cover technical guide: Addendum 2000.

Brownstein, G., Johns, C., Fletcher, A., Pritchard, D., & Erskine, P. D. (2015). Ecotones as indicators: boundary properties in wetland-woodland transition zones. Community ecology, 16(2), 235-243

Büttner, G., Kosztra, B., & Maucha, G. (2016). Accuracy Assessment of CLC Data. European landscape dynamics: CORINE land cover data, 41-52.

Coppin, P., Jonckheere, I., Nackaerts, K., Muys, B., & Lambin, E. (2004). Review article digital change detection methods in ecosystem monitoring: a review. International Journal of Remote Sensing, 25(9), 1565-1596.

Costa, R., Fraga, H., Fernandes, P., Fonseca, A., & Santos, J. (2018). Influence of precipitation variability in vegetation greenness in Portugal. *EGUGA*, 462.

Clark, J. R. (Ed.). (2018). Preface in *Coastal zone management handbook*. CRC press.

CLIMA, Portal do CLIMA. (2022). Alterações climáticas em Portugal. Disponível em http://portaldoclima.pt/ em fevereiro. accessed 17/02/2022.

Coltri, P. P., Ramirez, G. M., Walter, M. K. C., Zullo Junior, J., Pinto, H. S., Nascimento, C. R., Gonçalves, R. R. do V. (2009). *Utilização de índices de vegetação para estimativas não destrutivas da biomassa, estoque e seqüestro de carbono do cafeeiro Arábica*. Anais XIV Simpósio Brasileiro de Sensoriamento Remoto, INPE 25-30, 121-128.

Costa J.C. (2001) – *Tipos de vegetação e adaptações das plantas do litoral de Portugal continental*. In Albergaria Moreira, M.E., A. Casal Moura, H.M. Granja & F. Noronha (ed.) Homenagem (in honorio) Professor Doutor Soares de Carvalho. Braga. Universidade do Minho. 283-299.

Cover, C. L. (2018). Copernicus Land Monitoring Service.

da Rocha Almeida J. R., & da Silva Rocha, K. (2018). *Aplicação dos índices de vegetação NDVI, PRI, e CO2flux na caracterização da cobertura vegetativa da área de proteção ambiental Raimundo Irineu Serra.*

de Almeida, D. N. (2016). *Ecology and dynamics of Mediterranean saltmarshes in a perspective of habitat management and restoration policies: The cases of*

Alvor and Arade in Portugal (Doctoral dissertation, Universidade de Lisboa (Portugal)).

Dore, S., Kolb, T. E., Montes-Helu, M., Eckert, S. E., Sullivan, B. W., Hungate, B. A., Kaye, J. P., Hart, S. C., Koch, G. W., & Finkral, A. (2010). Carbon and water fluxes from ponderosa pine forests disturbed by wildfire and thinning. *Ecological Applications*, *20*(3), 663–683. https://doi.org/10.1890/09-0934.1 accessed 07/01/2020.

EEA-ETC/TE. 2002. CORINE land cover update. I&CLC2000 project. Technical guidelines, http://terrestrial.eionet.eu.int Access: 07/01/2021.

Eckert, S., Hüsler, F., Liniger, H., & Hodel, E. (2015). Trend analysis of MODIS NDVI time series for detecting land degradation and regeneration in Mongolia. *Journal of Arid Environments*, *113*, 16-28.

Ehlers, M., Sofina, N., Filippovska, Y., & Kada, M. (2014). Automated techniques for change detection using combined edge segment texture analysis, GIS, and 3D information. In Q. Weng (Ed.), Global urban monitoring and assessment through Earth observation (pp. 325–351). CRC Press, Taylor & Francis Group (Retrieved from http://www crcpress.com/product/isbn/9781466564497). Access: 23/02/2022.

Faracini, J. C. B. (2017). Técnicas de detecção remota na monitorização da vegetação e a contribuição da Ria Formosa no ciclo do carbono (Doctoral dissertation).

Feranec, J., Hazeu, G., Christensen, S., & Jaffrain, G. (2007). *Corine land cover change detection in Europe (case studies of the Netherlands and Slovakia). Land Use Policy, 24(1), 234–247.*

Fernandez, H. M., Granja-Martins, F. M., Pedras, C. M., Fernandes, P., & Isidoro, J. M. (2021). An Assessment of Forest Fires and CO2 Gross Primary Production from 1991 to 2019 in Mação (Portugal). Sustainability, 13(11), 5816.

Ferreira, V., Panagopoulos, T., Cakula, A., Andrade, R., & Arvela, A. (2015). Predicting Soil Erosion After Land Use Changes for Irrigating Agriculture in a Large Reservoir of Southern Portugal. *Agriculture and Agricultural Science Procedia*, *4*, 40–49.

Finlayson, C.M. and van der Valk, A.G. (1995): Wetlands classification and inventory: A summary. Vegetatio 118, pp. 185-192.

Forbrich, I., & Giblin, A. E. (2015). Marsh-atmosphere CO2 exchange in a New England salt marsh. *Journal of Geophysical Research G: Biogeosciences*, *120*(9), 1825–1838.

Folharini, S. O., & de Oliveira, R. C. (2017). Cálculo do Índice Espectral CO2FLUX em área de mata atlântica e sua relação com processos gravitacionais no município de Cubatão. Os Desafios da Geografia Física na Fronteira do Conhecimento, 1, 4642-4653.

Florenzano, T. G. (2002). Imagens de satélite para estudos ambientais. In Imagens de satélite para estudos ambientais (pp. 97-97).

Gaida, W., Breunig, F. M., Galvão, L. S., & Ponzoni, F. J. (2020). Correção Atmosférica em Sensoriamento Remoto: Uma Revisão. *Revista Brasileira de Geografia Física*, *13*(01), 229-248.

Gamon, J. A., Peñuelas, J., & Field, C. B. (1992). *A narrow-waveband spectral index that tracks diurnal changes in photosynthetic efficiency. Remote Sensing of Environment, 41(1), 35–44.*

Gamon, J. A., Penuelas, J., & Field, C. B. (1992). A narrow-waveband spectral

index that tracks diurnal changes in photosynthetic efficiency. Remote Sensing of Environment, 41(1), 35-44.

Guedes, J., & da Silva, S. M. P. (2018). Sensoriamento Remoto no estudo da vegetação: Princípios físicos, sensores e métodos. Acta Geográfica, 12(29), 127-144.

Gillespie, T. W., Ostermann-Kelm, S., Dong, C., Willis, K. S., Okin, G. S., & Macdonald, G. M. (2018). Monitoring changes of NDVI in protected areas of southern California NPS Landscape Dynamics Monitoring View project Biodiversity in Insular Environments View project Monitoring changes of NDVI in protected areas of southern California. *Ecological Indicators*, *88*, 485–494.

Gouveia, C., Trigo, R. M., & DaCamara, C. C. (2009). Drought and vegetation stress monitoring in Portugal using satellite data. *Natural Hazards and Earth System Science*, *9*(1), 185–195.

H., Gomes, C. P., & Martins, F. M. G. (2020). Monitorização por satélite da desflorestação da floresta do Maiombe em Cabinda, Angola nos últimos 33 anos. Revista Geama, 6(3), 81-91

Han, G., Chu, X., Xing, Q., Li, D., Yu, J., Luo, Y., Wang, G., Mao, P., & Rafique, R. (2015). Effects of episodic flooding on the net ecosystem CO2 exchange of a supratidal wetland in the Yellow River Delta. *Journal of Geophysical Research: Biogeosciences*, *120*(8), 1506–1520.

Hill, J., Stellmes, M., Udelhoven, T., Röder, A., & Sommer, S. (2008). Mediterranean desertification and land degradation. Mapping related land-use change syndromes based on satellite observations. *Global and Planetary Change*, *64*(3–4), 146–157.

Huang, S., Tang, L., Hupy, J. P., Wang, Y., & Shao, G. (2020). A commentary review on the use of normalized difference vegetation index (NDVI) in the era of popular Remote Sensing. Journal of Forestry Research, 1-6.

Ignácio de la Torre, José , Reconquista(2020) Trad. Diogo Costa. 1ª ed. Lisboa : Clube do Autor, 294, [1] p. : il. ; 23 cm. Tít. orig.: Breve historia de la Reconquista. ISBN 978-989-724-509-1.

Intergovernmental Panel on Climate Change (2013) Climate Change 2013: the physical science basis, summary for policymakers. WG1 contribution to IPCC AR5, 27 September 2013, 36 pp.

Instituto de Conservação da Natureza e da Floresta – ICNF (1991) *Revisão do Plano de Ordenamento do Parque da Ria Formosa, Vol I e II.*

Instituto de Conservação da Natureza e da Floresta - ICNF (2008) *Plano Setorial Rede Natural 2000.*

Instituto de Pesquisas Espaciais (INPE). Fundamentos Científicos das Mudanças Climáticas. São José dos Campos, SP: Rede Clima/INPE, 2012. 44 p. ISBN: 978-85-17-00064-5.

Justice, C. O., Townshend, J. R. G., Vermote, E. F., Masuoka, E., Wolfe, R. E., Saleous, N., ... & Morisette, J. T. (2002). An overview of MODIS Land data processing and product status. Remote Sensing of Environment, 83(1-2), 3-15.

Kriegler FJ, Malila WA, Nalepka RF, Richardson W (1969) Preprocessing transformations and their effect on multispectral recognition. Remote Sens Environ VI:97–132.Jung, M., & Chang, E. (2015). NDVI-based land-cover change detection using harmonic analysis. *International Journal of Remote Sensing*, *36*(4), 1097–1113.

Kombiadou, K., Matias, A., Ferreira, Ó., Carrasco, A. R., Costas, S., & Plomaritis,

T. (2019). Impacts of human interventions on the evolution of the Ria Formosa barrier island system (S. Portugal). *Geomorphology*, *343*, 129-144.

Kleemann, F., Lehner, H., Szczypińska, A., Lederer, J., & Fellner, J. (2017). Using change detection data to assess amount and composition of demolition waste from buildings in Vienna. *Resources, Conservation and Recycling*, *123*, 37–46.

Lourenço, P. M., Sousa, C. A., Seixas, J., Lopes, P., Novo, M. T., & Almeida, A. P. G. (2011). Anopheles atroparvus density modeling using MODIS NDVI in a former malarious area in Portugal. *Journal of Vector Ecology*, *36*(2), 279–291.

Liu, M., Zhu, R., Zhang, Z., Liu, L., Hui, R., Bao, J., & Zhang, H. (2016). *Water use traits and survival mechanisms of psammophytes in arid ecosystems. Arid Land Research and Management, 30(2), 166–180.* doi:10.1080/15324982.2015.1090498.

Lousã, M. (1986) – *Comunidades halofíticas da Reserva de Castro Marim*. Dissertação de Doutoramento. Instituto Superior de Agronomia.

Lu, D., Mausel, P., Brondizio, E., & Moran, E. (2004). Change detection techniques. International Journal of Remote Sensing, 25(12), 2365-2401.

Lule, A. V., & Vargas, R. (2018). Contrasting biophysical drivers of ecosystem-scale CO 2 and CH 4 fluxes across phenological phases in a tidal salt marsh. *AGUFM*, *2018*, B42C-03.

MAOTDR (2007) GIZC: bases para a Estratégia da Gestão integrada da Zona Costeira Nacional. [ICZM: Basis for a national strategy for integrated coastal zone management] Lisboa, Portugal: Ministério do Ambiente do Ordenamento do Território e do Desenvolvimento Regional.

Marcelo, M.J. & Cancela da Fonseca, L. (1998). *Ria Formosa: Da gestão e conservação de uma área protegida*. Revista de Biologia, 16,1-4:125-133.

Marcos, B., Gonçalves, J., Alcaraz-Segura, D., Cunha, M., & Honrado, J. P. (2019). Improving the detection of wildfire disturbances in space and time based on indicators extracted from MODIS data: a case study in northern Portugal. *International Journal of Applied Earth Observation and Geoinformation*, *78*, 77-85.

Markham, B. L., Storey, J. C., Williams, D. L., & Irons, J. R. (2004). Landsat sensor performance: history and current status. *IEEE Transactions on Geoscience and Remote Sensing*, *42*(12), 2691-2694.

Markham, B. L., & Helder, D. L. (2012). Forty-year calibrated record of earth-reflected radiance from Landsat: A review. *Remote Sensing of Environment*, *122*, 30-40.

Martins, F. M., Fernandez, H. M., Isidoro, J. M., Jordán, A., & Zavala, L. (2016). Classification of landforms in Southern Portugal (Ria Formosa Basin). *Journal of Maps*, *12*(3), 422-430.

Masek, J. G., Wulder, M. A., Markham, B., McCorkel, J., Crawford, C. J., Storey, J., & Jenstrom, D. T. (2020). Landsat 9: Empowering open science and applications through continuity. Remote Sensing of Environment, 248, 111968.

Melo, E. T., Sales, M. C. L., & Oliveira, J. G. B. (2011). Application of the normalized difference vegetation index (NDVI) in the analysis of the environmental degradation of the microbasin of Riacho dos Cavalos, Cratéus–CE. *RAEGA*, *23*, 520-533.

Meneses, P. R., & Almeida, T. D. (2012). Introdução ao processamento de imagens de sensoriamento remoto. Universidade de Brasília, Brasília.

Mitra S., Wassmann, R. & Vlek, P. (2003) *Global Inventory of Wetlands and their*

Role in the Carbon Cycle. ZEF – Discussion Papers on Development Policy No. 64, Center for Development Research, Bonn, pp. 44.

Middleton, E. M., Ungar, S. G., Mandl, D. J., Ong, L., Frye, S. W., Campbell, P. E., & Pollack, N. H. (2013). The earth observing one (EO-1) satellite mission: Over a decade in space. IEEE Journal of Selected Topics in Applied Earth Observations and Remote Sensing, 6(2), 243-256

Moffett, K. B., Wolf, A., Berry, J. A., & Gorelick, S. M. (2010). Saltmarsh–atmosphere exchange of energy, water vapor, and carbon dioxide: Effects of tidal flooding and biophysical controls. *Water Resources Research*,*46*(10). Moghaieb, R. E., Saneoka, H., & Fujita, K. (2004). Effect of salinity on osmotic adjustment, glycine betaine accumulation and the betaine aldehyde dehydrogenase gene expression in two halophytic plants, Salicornia europaea and Suaeda maritima. Plant science, 166(5), 1345-1349.

Monteith, J. L. (1977). Climate and the efficiency of crop production in Britain. Philosophical Transactions of the Royal Society of London. B, Biological Sciences, 281(980), 277-294.

Moura, D., Mendes, I., Aníbal, J., & Gomes, A. (2017). Guadiana River Estuary. Investigating the past, present and future.

Myneni, R. B., Los, S. O., & Asrar, G. (1995). *Potential gross primary productivity of terrestrial vegetation from 1982-1990. Geophysical Research Letters, 22(19), 2617–2620.* doi:10.1029/95gl02562

National Oceanic and Atmospheric Administration U.S. Department of Commerce (NOAA) (2017) available in: http://oceanservice.noaa.gov/facts/RemoteSensing.html. Access: 23/02/2021.

National Aeronautics and Space Administration, Science Mission Directorate. (2010). Visible Light. available in : http://science.nasa.gov/ems/09_visiblelight. Access: 02/03/2022

Nahrawi, H., Leclerc, M. Y., Zhang, G., & Pahari, R. (2017). Influence of Tidal Inundation on CO 2 Exchange between Salt Marshes and the Atmosphere. *Biogeosciences Discussions*, 1-27.

Novillo, C. J., Arrogante-Funes, P., & Romero-Calcerrada, R. (2019). Geo-Information Recent NDVI Trends in Mainland Spain: Land-Cover and Phytoclimatic-Type Implications. *Mdpi.Com*.

Oliveira, P. A. U. L. O. (2013). Considerações sobre o clima do Algarve. Direção Regional de Agricultura e Pescas do Algarve–Ministério da Agricultura, do Mar, do Ambiente e do Ordenamento do Território. Accessed in 02/10/2021. Available in http://www.drapalg.min-agricultura.pt/ . Access: 06/04/2020.

Ostermann, O. P. (1998). The need for management of nature conservation sites designated under Natura 2000. Journal of applied ecology, 35(6), 968-973.

Parente, J., Amraoui, M., Menezes, I., & Pereira, M. G. (2019). Drought in Portugal: Current regime, comparison of indices and impacts on extreme wildfires. *Science of the Total Environment*, *685*, 150–173.

Pedras, C. M. G., Valín, M. I., Fernandez, H., & Martins, F. M. G. (2014). Assessment of Soil Water Content and Remote Sensing Techniques-Case Study of Kiwi Orchard (Portugal). Journal of Agricultural Science and Technology A, 4(1), 33-42.

Pettorelli, N., Vik, J. O., Mysterud, A., Gaillard, J. M., Tucker, C. J., & Stenseth, N. C. (2005). Using the satellite-derived NDVI to assess ecological responses to environmental change. *Trends in Ecology and Evolution*, *20*(9), 503–510.

Pinto, C. T., Haque, M. O., Micijevic, E., & Helder, D. L. (2019). Pinto. *IEEE Transactions on Geoscience and Remote Sensing*, *57*(10), 7378-7394.

Poelking, E. L., Lauermann, A., & Dalmolin, R. (2007). Imagens CBERS na geração de NDVI no estudo da dinâmica da vegetação em período de estresse hídrico. Simpósio Brasileiro de Sensoriamento Remoto, 13, 21-26

Ponzoni, F. J., Antunes, M. A. H., Pinto, C. T., Lamparelli, R. A. C., & Junior, J. Z. (2015). Calibração de sensores orbitais. Oficina de Textos.

Rahman, A. F., Gamon, J. A., Fuentes, D. A., Roberts, D., Prentiss, D., & Qiu, H. (2000). Modelling CO2 flux of boreal forests using narrow-band indices from AVIRIS imagery. In AVIRIS Workshop.

Rahman, A. F., Gamon, J. A., Fuentes, D. A., Roberts, D. A., & Prentiss, D. (2001). Modelling spatially distributed ecosystem flux of boreal forest using hyperspectral indices from AVIRIS imagery. Journal of Geophysical Research: Atmospheres, 106(D24), 33579-33591

Raven, P. H. (2013). Biology of plants/Raven Biology of plants.

Rogan, J., Chen, D., 2004. Remote Sensing technology for mapping and monitoring land-cover and land-use change. Progress in Planning 61, 301–325.

Rodríguez, I., Montoya, I., Sánchez, M. J., & Carreño, F. (2009). Geographic information systems applied to integrated coastal zone management. Geomorphology, 107(1-2), 100-105.

Rouse Jr, J. W., Haas, R. H., Deering, D. W., Schell, J. A., & Harlan, J. C. (1974). Monitoring the Vernal Advancement and Retrogradation (Green Wave Effect) of Natural Vegetation. [Great Plains Corridor]

Roy, P. S. (1989). Spectral reflectance characteristics of vegetation and their use in estimating productive potential. Proceedings: Plant Sciences, 99(1), 59-81.

Roy, D. P., Wulder, M. A., Loveland, T. R., Woodcock, C. E., Allen, R. G., Anderson, M. C., ... & Zhu, Z. (2014). Landsat-8: Science and product vision for terrestrial global change research. *Remote sensing of Environment*, *145*, 154-172.

Sá, A. F. F. D. (2012). *Rede de percursos de natureza da Reserva Natural do Sapal de Castro Marim e Vila Real de Santo António* .

Sabins, F. F. (2007). Remote Sensing: principles and applications. Waveland Press.

Serrano-Ortiz, P., Were, A., Reverter, B. R., Villagarcía, L., Domingo, F., Dolman, A. J., & Kowalski, A. S. (2015). Seasonality of net carbon exchanges of Mediterranean ecosystems across an altitudinal gradient. *Journal of Arid Environments*, *115*, 1–9.

Savtchenko, A., Ouzounov, D., Ahmad, S., Acker, J., Leptoukh, G., Koziana, J., & Nickless, D. (2004). Terra and Aqua MODIS products available from NASA GES DAAC. Advances in Space Research, 34(4), 710-714.

Sellers, P. J. (1987). Canopy reflectance, photosynthesis, and transpiration, II. The role of biophysics in the linearity of their interdependence. Remote Sensing of Environment, 21(2), 143-183.

Schmidt, M. W., & Noack, A. G. (2000). Black carbon in soils and sediments: analysis, distribution, implications, and current challenges. Global biogeochemical cycles, 14(3), 777-793.

Silveira, E. M. de O., Acerbi Júnior, F. W., Mello, J. M. de, & Bueno, I. T. (2017). Object-based change detection using semivariogram indices derived from NDVI images: The environmental disaster in Mariana, Brazil. *Ciência e Agrotecnologia*, *41*(5), 554–564.

Stathopoulou, M., Cartalis, C., & Keramitsoglou, I. (2004). Mapping micro-urban heat islands using NOAA/AVHRR images and CORINE Land Cover: an application to coastal cities of Greece. International Journal of Remote Sensing,

Suess, S., Van der Linden, S., Okujeni, A., Griffiths, P., Leitão, P. J., Schwieder, M., & Hostert, P. (2018). Characterizing 32 years of shrub cover dynamics in southern Portugal using annual Landsat composites and machine learning regression modeling. *Remote Sensing of Environment*, *219*, 353–364. https://doi.org/10.1016/j.rse.2018.10.004.

Sun, C., Fagherazzi, S., & Liu, Y. (2018). Classification mapping of salt marsh vegetation by flexible monthly NDVI time-series using Landsat imagery. *Estuarine, Coastal and Shelf Science*, *213*, 61–80.

Susano, C. L., & Gonçalves, M. M. (2020).SALT: THE WHITE GOLD OF ALGARVE.

Teillet, P. M., & Ren, X. (2008). Spectral band difference effects on vegetation indices derived from multiple satellite sensor data. *Canadian Journal of Remote Sensing*, *34*(3), 159-173.

Teodoro, A., & Amaral, A. (2019). A Statistical and Spatial Analysis of Portuguese Forest Fires in Summer 2016 Considering Landsat 8 and Sentinel 2A Data. *Environments*, *6*(3), 36.

Tewkesbury, A. P., Comber, A. J., Tate, N. J., Lamb, A., & Fisher, P. F. (2015). A critical synthesis of Remotely sensed optical image change detection techniques. Remote Sensing of Environment, 160, 1-14.

Tuia, D., Persello, C., & Bruzzone, L. (2016). Domain adaptation for the classification of Remote Sensing data: An overview of recent advances. *IEEE Geoscience and Remote Sensing Magazine*, *4*(2), 41–57.

Treitz, P., & Rogan, J. (2004). Remote Sensing for mapping and monitoring land-cover and land-use change-an introduction. Progress in planning, 61(4), 269-279.

Usman, M., Liedl, R., Shahid, M. A., & Abbas, A. (2015). Land use/land cover classification and its change detection using multi-temporal MODIS NDVI data. *Journal of Geographical Sciences*, *25*(12), 1479–1506.

Vaz, E. M. D. N. (2011). Regional change in the Algarve: A Geographic Information System approach.

Veloso-Gomes, F., Barroco, A., Pereira, A. R., Reis, C. S., Calado, H., Ferreira, J. G., ... & Biscoito, M. (2008). Basis for a national strategy for integrated coastal zone management—in Portugal. *Journal of Coastal Conservation*, *12*(1), 3-9.

Vermote, A. F., & Kumar, L. (2019). An assessment of the impact of urbanization and land-use changes in the fast-growing cities of Saudi Arabia Modeling soil erosion in the Nepal Himalayas using models, GIS and Remote Sensing View project An assessment of the impact of urbanization and land-use changes in the fast-growing cities of Saudi Arabia * An assessment of the impact of urbanization and land-use changes in the fast-growing cities of Saudi Arabia. *Taylor & Francis*, *34*(1), 78–97.

Viana, C. M., Girão, I., & Rocha, J. (2019). Long-Term Satellite Image Time-Series for Land Use/Land Cover Change Detection Using Refined Open Source Data in a Rural Region. *Mdpi.Com*.

Viegas, C. (2011). *A ocupação romana do Algarve: estudo do povoamento e economia do Algarve central e oriental no período romano*. Uniarq.

Vicente-Serrano, S. M., Gouveia, C., Camarero, J. J., Beguería, S., Trigo, R.,

López-Moreno, J. I., Azorín-Molina, C., Pasho, E., Lorenzo-Lacruz, J., Revuelto, J., Morán-Tejeda, E., & Sanchez-Lorenzo, A. (2013). Response of vegetation to drought time-scales across global land biomes. *Proceedings of the National Academy of Sciences of the United States of America*, *110*(1), 52–57.

Wang, J., Chen, Y., Chen, F., Shi, T., & Wu, G. (2018). Wavelet-based coupling of leaf and canopy reflectance spectra to improve the estimation accuracy of foliar nitrogen concentration. *Agricultural and Forest Meteorology*, *248*, 306-315.

Xu, L., Li, B., Yuan, Y., Gao, X., Zhang, T., & Sun, Q. (2016). Detecting different types of directional land cover changes using MODIS NDVI time series dataset. *Remote Sensing*, *8*(6), 495.

Xue J, Su B (2017) Significant Remote Sensing vegetation indices: a review of developments and applications. J Sensors 2017:1–17

Zachar, D. (1982). Soil erosion. Developments in Soil Science 10. Amsterdam: Elsevier

Zanter, K. (2016). Landsat 8 (L8) data users handbook. *Landsat Science Official Website*

Zhu, Z. (2017). Change detection using landsat time series: A review of frequencies, preprocessing, algorithms, and applications. *ISPRS Journal of Photogrammetry and Remote Sensing*, *130*, 370-384.